DETERMINATION OF TEMPERATURE PROFILE IN QUENCHING BY NUMERICAL METHODS AND VERIFICATION BY EXPERIMENTS

by
H. K. KANODIA

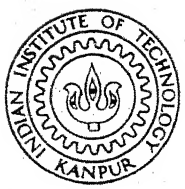

Department of Mechanical Engineering
INDIAN INSTITUTE OF TECHNOLOGY
KANPUR
JULY 1978

DETERMINATION OF TEMPERATURE PROFILE IN QUENCHING BY NUMERICAL METHODS AND VERIFICATION BY EXPERIMENTS

A Thesis Submitted in
Partial Fulfilment of the Requirements
for the Degree of
MASTER OF TECHNOLOGY

by
H. K. KANODIA

to the

Department of Mechanical Engineering
INDIAN INSTITUTE OF TECHNOLOGY
KANPUR
JULY 1978

CERTIFICATE

This is to certify that the thesis entitled "Determination of Temperature Profile in Quenching by Numerical Methods and Verification by Experiments" is a record of work carried out by Mr. Hemant Kumar Kanodia under my supervision and that it has not been submitted elsewhere for a degree.

J. Srinivasan

Dr. J.Srinivasan
Assistant Professor
Department of Mechanical Engineering
Indian Institute of Technology
Kanpur

ACKNOWLEDGEMENTS

I express my sincere gratitude to Dr. J. Srinivasan, my supervisor for his constant encouragement, invaluable guidance, comments and criticism throughout the tenure of this work.

I am thankful to Mr. V.K. Agrawal, Mr. S.K. Urmalia, Mr. R.S. Tomar, Mr. R.K. Sheogaonkar and all other my friends for their timely help and cooperation.

The typing by Mr. K.N. Tewari is appreciated.

July 1978. H.K. Kanodia

CONTENTS

LIST OF FIGURES

LIST OF TABLES

NOMENCLATURE

A	Constant of integration.
b_M	A factor.
B	Constant of integration.
Bi	Biot number (hL/K or hR/K).
f	Kernel defined by eqn.(3.11).
fa	Approximated kernel defined by eqn. (3.13).
f(t)	Function of t.
F(s)	Laplace image function of f(t).
Fo	Fourier number ($\alpha t/L^2$ or $\alpha t/R^2$).
h	Surface heat transfer coefficient, W/m^2-°K.
$\bar{h}$	Nondimensional surface heat transfer coefficient.
I_n	Modified Bessel's function of 1st kind and nth order.
J_n	Bessel's function of 1st kind and nth order.
K	Conduction heat transfer coefficient, W/m-°K.
K_n	Modified Bessel's function of 2nd kind and nth order.
L	Half thickness of the plate, m.
m	A variable.
M	A constant.
M_0,M_1	Constants of kernel property defined by eqns. (3.20) and (3.21) respectively.
n	A variable.
N	Constant of Gaussian integration formula.
q	Heat flux at surface, W/m^2.
$\bar{q}$	Laplace image of q.

r	Variable of cylinderical coordinate, m.
$r(s)$	Function of s.
$\bar{r}$	Dimer ionless cylinderical coordinate.
R	Radius of infinite, cylinder, m.
s	Variable of Laplacé transform.
t	Time, sec.
t_m	Nondimensional time.
T	Temperature, °K.
$w_i^{(2N)}$	Gaussian weightage of order (2N).
x	Variable of Cartesian coordinate, m.
$\bar{x}$	Dimensionless cartesian coordinate variable.
x_i	Coordinate of Gaussian integration formula.
α	Thermal diffisivity, m^2/sec.
α_n	nth zero of a function r(s), eqn.(A2.4).
β_M	Multiplication factor of Mth term, eqn.(2.37).
ε_M	Multiplication factor of Mth term, eqn.(3.13).
θ	Dimensionless temperature defined by eqn.(2.8a).
$\bar{\theta}$	Laplace image of θ .
$\theta_n(\mu)$, $\theta_n(\mu/\tau)$	Theta functions defined by eqn.(2.22).
$\theta_n(x,\tau)$	Dimensionless temperature, (n+1)th term in expansion of θ, eqn.(3.15).
∇	Laplacian operator.
$\mathcal{L}$	Operator of Laplace transform.

μ_n nth Eigenvalue, eqn.(2.37).

τ Dummy variable of definite integral.

τ_i Time coordinate corresponding to Gaussian coordinate, x_i.

Superscript

$'$ Used in Poisson summation formula, eqn.(A3.1), to indicate that the first term is half than the normal value.

$'$ Derivatives.

Subscript

i Corresponds to initial value.

f Corresponds to fluid.

k Corresponds to kth term.

m Corresponds to mth term.

M Corresponds to mth term.

n Corresponds to nth term.

ref Corresponds to reference value.

SYNOPSIS

DETERMINATION OF TEMPERATURE PROFILES IN QUENCHING BY NUMERICAL METHODS AND VERIFICATION BY EXPERIMENTS

H.K. Kanodia

Master of Technology
Department of Mechanical Engineering
Indian Institute of Technology, Kanpur

The present work is concerned with the prediction of temperature profile during the quenching of a material. The surface heat transfer coefficient during quenching vary significantly in the film boiling and nucleate boiling regim and also depends strongly on the temperature difference. Hence the problem for one dimensional heat conduction reduces to the solution of a partial differential equation in two variables with a nonlinear boundary condition. This is converted to nonlinear singular Volterra integral equation. The integral equation is solved numerically by two methods - the successive iteration and separable kernel method. The numerical solutions are compared with experimental results and results available in the literature. It is shown that the separable kernel method is more accurate if sufficiently large number of terms are considered in the expansion of the singular kernel.

CHAPTER 1

INTRODUCTION

Heat treatment is an important method used in industries to increase the quality, reliability and durability of engineering components by imparting the desired mechanical properties. The desired mechanical properties can be increased hardness, wear resistance, ductility, toughness etc. Heat treatment processes can be broadly classified into the following categories:

1. Thermal Treatments: Where there is a change in type and proportions of phases present in the solid or concentration and distribution of crystal defects.
2. Thermochemical Treatments : Where there is a change in chemical composition of surface layers (e.g. carburising and nitriding).

The thermal treatments can be subdivided into four sections depending upon the structure resulting from the treatments. They are:

a) Annealing: Heating to and holding at a suitable temperature and then cooling at a suitable rate, for such purposes as reducing hardness, improving machinability, facilitating cold working etc.

b) Quenching: Hardening a ferrous alloy by heating it above the phase transformation temperature and then cooling rapidly so that some or all of the austenite transforms to martensite.

c) Tempering: Reheating a quenched hardened alloy to a temperature below the transformation range and then cooling at any desired rate.

d) Aging: A change in the properties of certain metals that occurs at ambient or moderately elevated temperatures.

The main aim of quenching and tempering is to increase the hardness and wear resistance, retaining a sufficient toughness at the same time. Quench hardening is discussed in detail hereafter.

As mentioned above, quench hardening is one of the thermal heat treatment processes, where concentration and distribution of crystal defects play an important role. The mechanical properties of a crystal are determined by the number and mobility of dislocations contained in them. Point defects exist in crystals in thermal equilibrium and may contribute to mechanical properties through diffusion, however, remarkable effects are caused by nonequilibrium concentration of point defects. If this nonequilibrium concentration of point defects is achieved by rapid cooling from high temperatures, the resulting hardening is called "quench hardening".

Hardening in the ferrous alloys is a result of supercooled transformation of phase. This can be explained by cooling curves on TTT (time, temperature and transformation) diagram, Fig.1. The TTT diagram is a curve, which gives the percentage and structure of decomposed austenite corresponding to the temperature and time. If components are cooled rapidly, austenite does not have enough time to decompose at a high temperature with the formation of ferrite-cementite mixture. It is supercooled and is transformed into martensite. Martensite is a hardened steel structure.

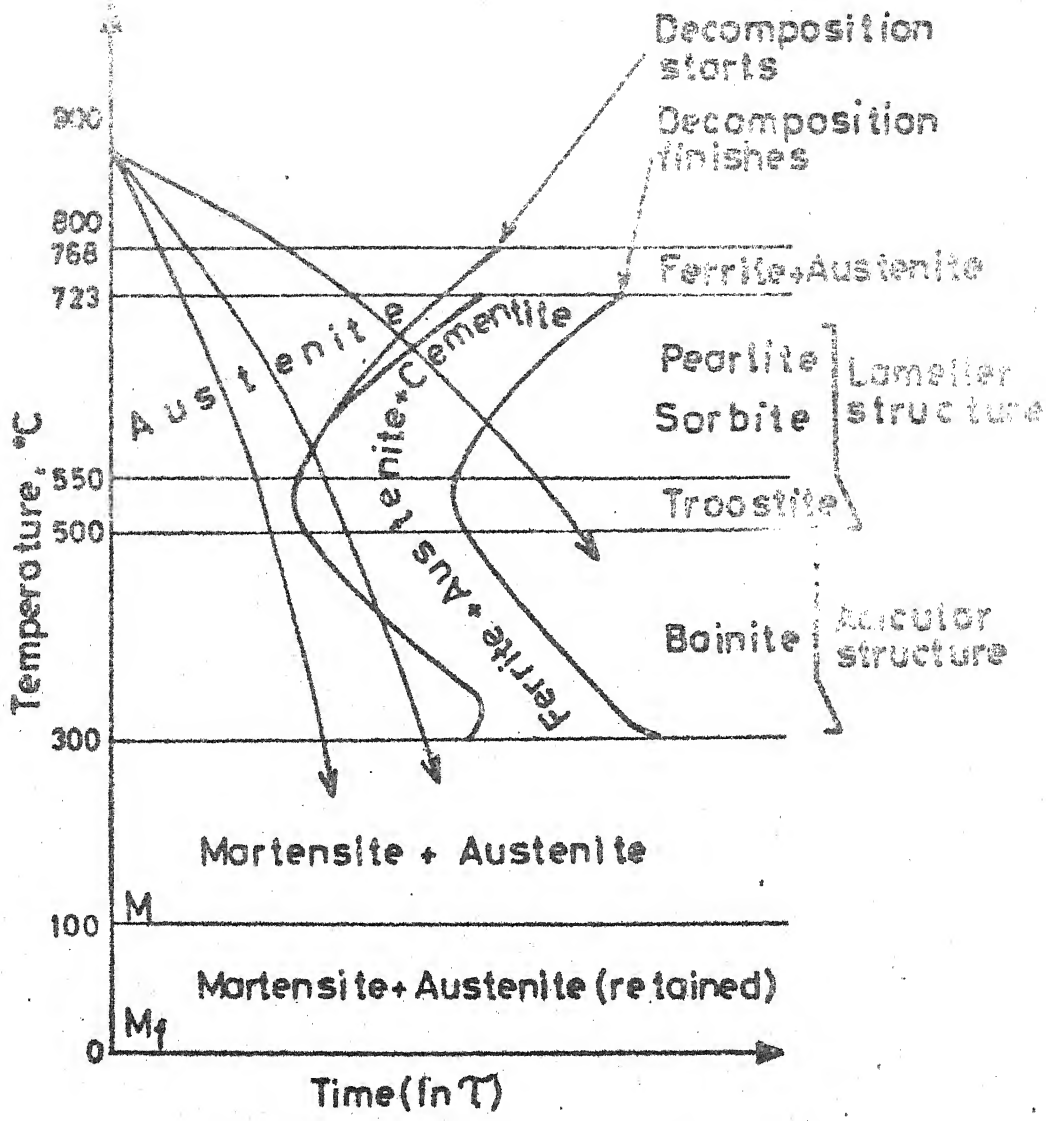

Fig.1 Cooling curves on time, temperature and transformation (TTT) diagram

The most extensively used method for hardening is quenching in a single medium. The main disadvantage of this method is crack formation due to simultaneous influence of transformation stresses and thermal stresses (caused by high rates of cooling in the temperature range of martensite formation). Hence, sometimes two quenching media are used. The second quenching media is less intensive. When the component is transferred from one quenching media to another quenching media, it may or may not be held at a constant temperature for sometime (Fig.2).

For a given design of a component, factors like nature and number of quenching media, initial temperature of the component, temperature of quenching media and holding time in quenching media, depend upon the material chosen and desired mechanical properties. All this requires an extensive knowledge of the rate of cooling of both the surface and interior of the component during quenching.

In quenching,heat flows from component to the quenching media at the interface, known as surface. Heat transfer at the surface mainly occurs by convection and/or by radiation. For unsteady convective heat transfer, boundary conditions of the fourth kind is used i.e., the interface temperature of both the media and component are same and boundary layer theory is applied. If the quenching media is large its temperature can be considered uniform and heat flux is proportional to the excess-temperature(-- over fluid temperature). The proportionality constant is known as surface heat transfer coefficient which may be a function of excess temperature.

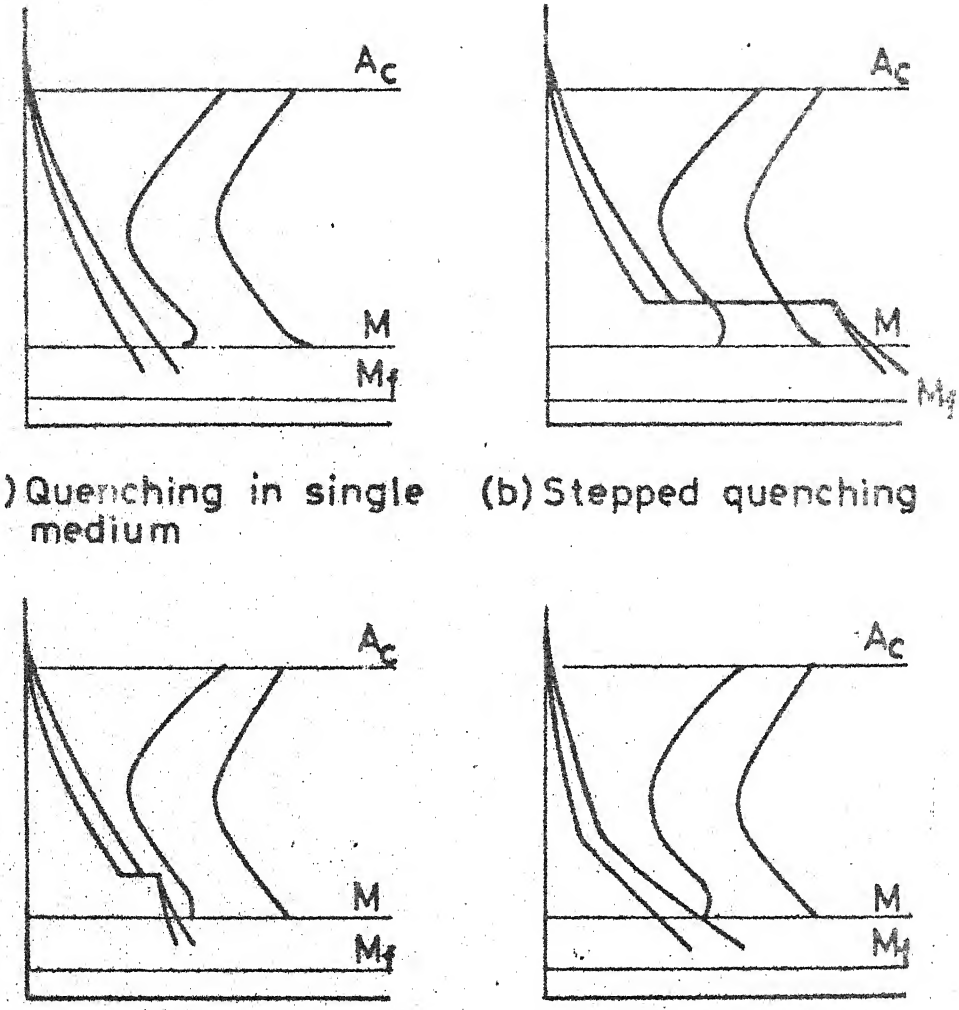

(a) Quenching in single medium

(b) Stepped quenching

(c) Isothermal quenching

(d) Quenching in two medium without time lag

A_c - Recrystalisation temperature
M - Martensite formation - STARTS
M_f - Martensite formation - STOPS

Fig. 2 Methods of quenching

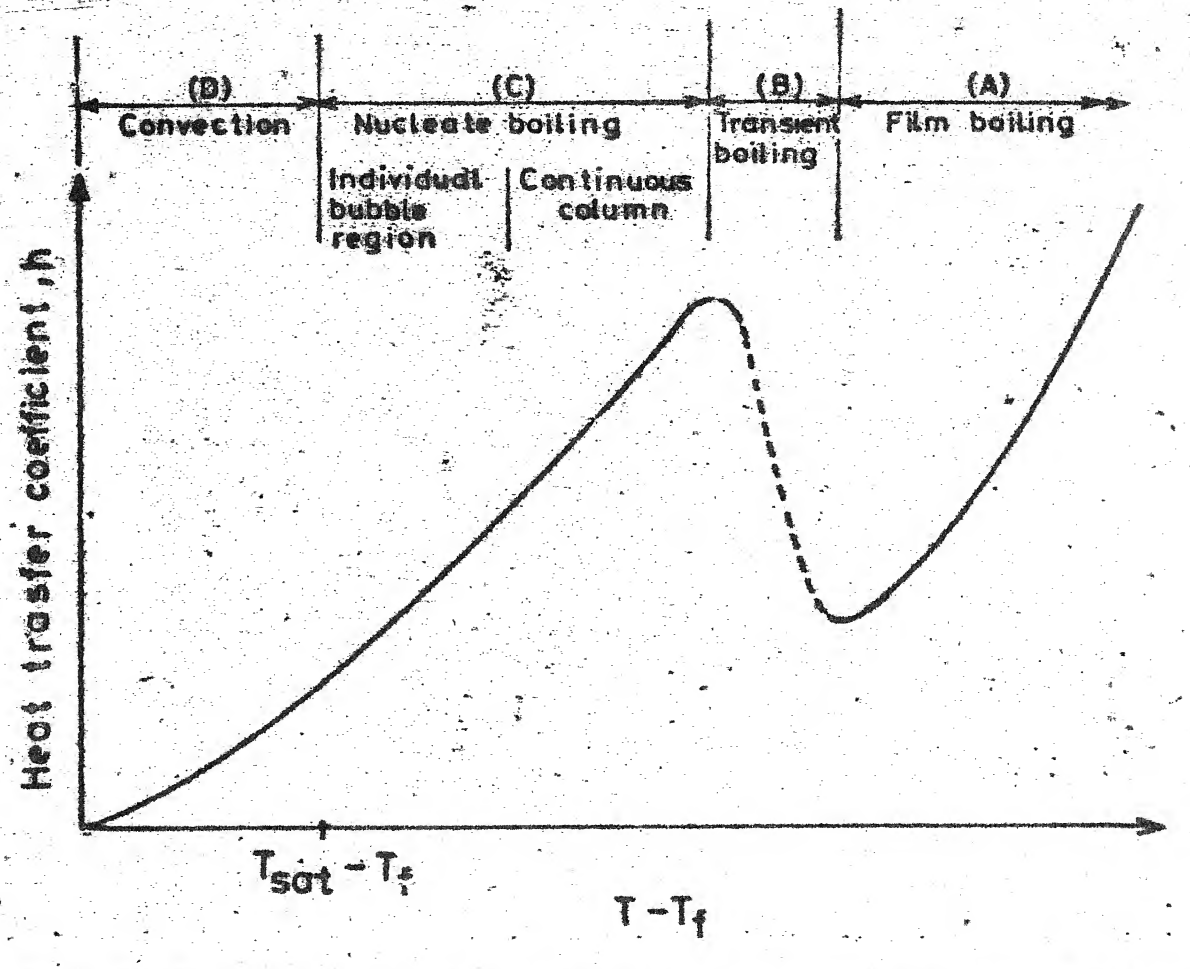

Fig.3 Typical cooling curve for a pool boiling

As shown in the plot (Fig.3), heat transfer coefficient is a strong function of excess temperature of surface. The entire region may be divided into four distinct stages of different intensity:

a) At the first stage (Region A) a thin vapour film surrounds the hot metal. Cooling proceeds by film boiling. Cooling rate is slow and is determined mainly by radiation.

b) In this region (Region B) cooling proceeds by transition boiling, a stage in between the film boiling and nucleate boiling.

c) The vapour film breaks up and liquid boils with bubble formation on the surface of the metal being cooled. Since all cooling is accomplished by vapour generation, this is the fastest stage of cooling, known as nucleate boiling (Region C).

d) Below saturation temperature, cooling is much slower as heat is extracted mainly by convection (Region D).

The earliest analytical work for transient cooling was done by Fourier (1878) with simplest boundary conditions, namely of constant surface heat transfer coefficient. Results of this work have been tabulated and plotted for practical use by Curney-Lurie (1923) and Heisler (1947). Though these results are presented for one dimensional heat flow only, these can be extended to three dimensional heat flow also.

In hardening, cooling proceeds through all stages of heat removal. Hence surface heat transfer coefficient changes rapidly as surface temperature goes down. Hence, analysis given by Fourier (1878) cannot be applied directly. In order to use Heisler charts we need to

assume some average constant heat transfer coefficient. However, there is no guide-line for the choice of this average heat transfer coefficient.

For obtaining detailed history of temperature at any time and coordinate during quenching, one has to go for mathematical analysis. The problem of transient heat conduction in a solid with surface heat flux as a function of temperature is a nonlinear problem. The nonlinear transient heat conduction problem can be reduced to the solution of a nonlinear singular Volterra integral equation. Numerical methods are used to overcome the nonlinearity and singularity.

The present study is concerned with a general nonlinear transient heat conduction problem resulting from a nonlinear surface flux. In general, solid is subjected to surface heat flux varying with various stages of boiling and natural convection.

While the literature dealing with the particular cases of convection, radiation is extensive, the unsteady problem of heat conduction with varying heat flux at surface due to various boiling stages has received little attention. Transient heat conduction in a plate subjected to pure thermal radiation on one face and combined forced convection and radiation on the other has been studied by Burka (1966). The problem was reduced to the solution of two simultaneous singular nonlinear Volterra integral equations. The two equations were replaced by a system of nonlinear algebraic equations and were solved for one set of parameters over a limited time range.

Crosbie and Viskanta (1966) presented an iterative numerical technique for solving nonlinear Volterra integral equations. The same method was applied to solve the problem of transient heating or cooling of a plate by combined convection and radiation (1968a). They compared their results for one set of parameters with the results of Vidin and Ivanov (1965) and results obtained by finite difference method.

Vidin and Ivanov (1965) transformed the linear energy equation and nonlinear boundary conditions into a nonlinear partial differential equation with a linear boundary condition. The resulting nonlinear partial differential equation was solved approximately by iteration.

A simplified method which approximates the kernel of integral equation by a separable kernel has also been presented by Crosbie and Viskanta (1968b). This method was improved and applied to transient cooling of sphere in oil by Crosbie and Banerjee (1973,1974).

The present work is concerned with the development of a computer programme for obtaining the history of temperature vs. time plot for a quenched component. The computer may be regarded as a simulator and is used in the same manner as an experimental rig of great flexibility in which the effect of changes in different parameters may be investigated. A quenching process can be finalised with some certainty before we go for actual testing, with their problems of high cost and time delay.

Some experiments have also been performed and results compared with numerical solutions. Although, because of laboratory limitations, experiments for very high initial body temperature could not be performed.

The present work can be extended for different positions of components. Also, one may consider the variation of heat transfer coefficient with the coordinates. Though, this will be highly nonlinear problem. Complicated shapes, other than infinite plate, infinite cylinder and sphere, have to be solved by finite element method or finite difference method.

CHAPTER 2

ANALYTICAL FORMULATION

In the present work only one dimensional geometries are considered. Physical and mathematical models for infinite plate and infinite cylinder have been considered and their solutions discussed here.

2.1 INFINITE PLATE

2.1.1 PHYSICAL MODEL:

Consider a slab of thickness 2L with uniform initial temperature, T_i. The slab is suddenly quenched in a cooling medium (also known as quenchent) at temperature T_f, such that $T_f < T_i$. The following assumptions are made in the analysis:

1. The conduction heat transfer is one dimensional.
2. The plate is isotropic, homogeneous and opaque to thermal radiation.
3. The physical properties are independent of temperature.
4. Quenching media temperature is not a function of time.

and 5. The plate does not contain any heat sources or sinks.

2.1.2 MATHEMATICAL MODEL:

The governing differential equation

$$\frac{\partial T(x,t)}{\partial t} = \alpha \nabla^2 T(x,t) \qquad (2.1)$$

reduces to

$$\frac{\partial T(x,t)}{\partial t} = \alpha \frac{\partial^2 T(x,t)}{\partial x^2} \qquad (2.2)$$

for one dimensional heat flow. This partial differential equation has two boundary conditions and an initial condition. As problem is symmetric about the center plane, which is the origin of the coordinate system, the boundary conditions at x = 0 and x = L are

$$\frac{\partial T(0,t)}{\partial x} = 0 \qquad (2.3a)$$

$$\frac{\partial T(L,t)}{\partial x} = -\frac{q\{T(L,t)\}}{K} \qquad (2.3b)$$

and initial condition is

$$T(x,0) = T_i \qquad (2.4)$$

First boundary condition (2.3a), specifies that the temperature gradient at the center is zero, while second boundary condition (2.3b), is a statement of energy balance at the surface. To simplify the analysis, eqn.(2.2) is non-dimensionalised in terms of dimensionless variables and then the eqn.(2.2), reduces to

$$\frac{\partial\theta(\bar{x}, Fo)}{\partial Fo} = \frac{\partial\theta(\bar{x}, Fo)}{\partial \bar{x}^2} \qquad (2.5)$$

while the boundary conditions and initial condition reduce to

$$\frac{\partial\theta(0, Fo)}{\partial \bar{x}} = 0 \qquad (2.6a)$$

$$\frac{\partial\theta(1, Fo)}{\partial \bar{x}} = -\frac{q\{\theta(1, Fo)\}L}{K} \qquad (2.6b)$$

and $$\theta(\bar{x}, 0) = 1 \qquad (2.7)$$

where

$$\theta = \frac{T - T_f}{T_i - T_f} \tag{2.8a}$$

$$\bar{x} = \frac{x}{L} \tag{2.8b}$$

$$Fo = \frac{\alpha t}{L^2} \tag{2.8c}$$

2.1.3 SOLUTION TO THE PARTIAL DIFFERENTIAL EQUATION:

Since the second boundary condition (2.6b) is nonlinear, none of the conventional methods are useful for solving the above partial differential equation (2.5). This equation can be reduced to a non-linear, singular Volterra integral equation by different methods, as shown by Luikov (1968). In the present work this equation is solved by Laplace Transform method.

Taking the Laplace Transform with respect to the variable Fo, partial differential equation (2.5), reduces to a total differential equation

$$s\,\bar{\theta}(\bar{x}, s) - \theta(\bar{x}, 0) = \frac{d^2\bar{\theta}(\bar{x}, s)}{d\bar{x}^2} \tag{2.9}$$

where

$$\bar{\theta}(\bar{x}, s) = \int_0^\infty \exp(-s\,Fo)\,\theta(\bar{x}, Fo)\,d\,Fo \tag{2.10}$$

Boundary conditions (2.6), can be written as follows:

$$\frac{d\bar{\theta}(0, s)}{d\bar{x}} = 0 \tag{2.11a}$$

and

$$\frac{d\bar{\theta}(1, s)}{d\bar{x}} = -\frac{\bar{q}\{\bar{\theta}(1, s)\}\cdot L}{K} \tag{2.11b}$$

Substituting the value of $\theta(\bar{x}, 0)$ in total differential equation (2.9), from initial condition (2.7) and rearranging the equation, we get

$$\frac{d^2 \bar{\theta}(\bar{x}, s)}{d\bar{x}^2} - s\,\bar{\theta}(\bar{x}, s) = -1 \qquad (2.12)$$

General solution of this equation is

$$\bar{\theta}(\bar{x}, s) = A \exp(\sqrt{s}\,\bar{x}) + B \exp(-\sqrt{s}\,\bar{x}) + \frac{1}{s} \qquad (2.13)$$

where A and B are arbitrary integration constants. Using boundary conditions (2.11), for finding the values of A and B, general solution can be written as

$$\bar{\theta}(\bar{x}, s) = -\frac{\bar{q}\{\bar{\theta}(1,s)\}L}{K}\,\frac{1}{\sqrt{s}}\,\frac{\exp(\sqrt{s}\,\bar{x})+\exp(-\sqrt{s}\,\bar{x})}{\exp(\sqrt{s}) - \exp(-\sqrt{s})} + \frac{1}{s} \qquad (2.14)$$

or

$$\bar{\theta}(\bar{x}, s) = -\frac{\bar{q}\{\bar{\theta}(1, s)\}L}{K}\,\frac{1}{\sqrt{s}}\,\frac{\cosh \bar{x}\sqrt{s}}{\sinh\sqrt{s}} + \frac{1}{s} \qquad (2.15)$$

Using the relation from Laplace inversion tables given by Doetsch (1961),

$$\mathcal{L}^{-1}\left[\frac{\cosh \bar{x}\sqrt{s}}{\sqrt{s}\sinh\sqrt{s}}\right] = 1 + 2\sum_{n=1}^{\infty} \exp(-n^2\pi^2 Fo)\cos\{2n\pi(\frac{\bar{x}+1}{2})\} \qquad (2.16)$$

and using convolution theorem, general solution of differential equation (2.15) can be written as

$$\theta(\bar{x}, Fo) = 1 - \frac{L}{K}\int_0^{Fo}\left[1+2\sum_{n=1}^{\infty}\exp\{-n^2\pi^2(Fo-\tau)\}\cos\{n\pi(\bar{x}+1)\}\right] q\{\theta(1,\tau)\}\,d\tau \qquad (2.17)$$

or

$$\theta(\bar{x}, Fo) = 1 - \frac{1}{K}\int_0^{Fo} [1+2\sum_{n=1}^{\infty}(-1)^n \cos(n\pi\bar{x})\exp\{-n^2\pi^2(Fo-\tau)\}]$$

$$h\ \theta(1,\tau)\}\theta(1,\tau)\,d\tau \qquad (2.18)$$

where h is heat transfer coefficient, it may be written as

$$q\{\theta(1,\tau)\} = h\{\theta(1,\tau)\}\theta(1,\tau) = h_{ref}\,\bar{h}\{\theta(1,\tau)\}\theta(1,\tau) \qquad (2.19)$$

where h_{ref} is a reference heat transfer coefficient. It may be an initial heat transfer coefficient or a maximum heat transfer coefficient, whichever is convenient. $\bar{h}$ is a nondimensional parameter. Substituting h by $h_{ref}\ \bar{h}$ in eqn.(2.18), we get

$$\theta(\bar{x}, Fo) = 1 - Bi_{ref}\int_0^{Fo} [1+2\sum_{n=1}^{\infty}(-1)^n\cos(n\pi\bar{x})\exp\{-n^2\pi^2(Fo-\tau)\}]$$

$$\bar{h}\{\theta(1,\tau)\}\theta(1,\theta)\,d\tau \qquad (2.20)$$

where Bi_{ref} is Biot no. corresponding to reference heat transfer coefficient. This integral equation is a nonlinear, singular Volterra integral equation and for surface this equation reduces to

$$\theta(1,Fo) = 1 - Bi_{ref}\int_0^{Fo} [1+2\sum_{n=1}^{\infty}\exp\{-n^2\pi^2(Fo-\tau)\}]\ \bar{h}\{\theta(1,\tau)\}$$

$$\theta(1,\tau)\,d\tau \qquad (2.21)$$

The kernel within the integral sign of eqn.(2.20) is known as Theta function θ_4 (Appendix I).

$$\theta_4\left(\frac{\pi x}{2}\right) = 1+2\sum_{n=1}^{\infty}(-1)^n\cos(n\pi\bar{x})\exp\{(n^2\pi^2(Fo-\tau)\} \qquad (2.22)$$

2.2 INFINITE CYLINDER

2.2.1 PHYSICAL MODEL:

Consider a cylinder of diameter 2R and uniform initial temperature T_i. The cylinder is suddenly dipped in a quenchent at temperature T_f, such that $T_f < T_i$. Same assumptions are made as in the case of slab (article 2.1.1) and similar analysis is done for cylinder.

2.2.2 MATHEMATICAL MODEL:

The governing differential heat flow equation

$$\frac{\partial T(r, t)}{\partial t} = \alpha \nabla^2 T(r, t) \qquad (2.23)$$

reduces to a nondimensional form

$$\frac{\partial \theta(\bar{r}, Fo)}{\partial Fo} = \frac{\partial^2 \theta(\bar{r}, Fo)}{\partial \bar{r}^2} + \frac{1}{\bar{r}} \frac{\partial \theta(\bar{r}, Fo)}{\partial \bar{r}} \qquad (2.24)$$

for one dimensional heat conduction. Boundary conditions are

$$\frac{\partial \theta(0, Fo)}{\partial \bar{r}} = 0 \qquad (2.25a)$$

$$\frac{\partial \theta(1, Fo)}{\partial \bar{r}} = -\frac{q\{\theta(1, Fo)\} R}{K} \qquad (2.25b)$$

and initial condition is

$$\theta(\bar{r}, 0) = 1 \qquad (2.26)$$

where $$\bar{r} = r/R \qquad (2.27)$$

This eqn. (2.24) with nonlinear boundary condition (2.25b) is also solved by Luikov (1968), but here it is solved by using Laplace Transform method.

Taking Laplace transform of eqn. (2.24) with respect to the variable Fo and using initial condition (2.26), partial differential equation reduces to total differential equation

$$\frac{d^2\bar{\theta}(\bar{r}, s)}{d\bar{r}^2} + \frac{1}{\bar{r}} \frac{d\bar{\theta}(\bar{r},s)}{d\bar{r}} - s\,\bar{\theta}(\bar{r},s) = -1 \qquad (2.28)$$

The general solution to the eqn.(2.28) is written as

$$\bar{\theta}(\bar{r}, s) = A\ I_o(\bar{r}\sqrt{s}) + B\,K_o(\bar{r}\sqrt{s}) + \frac{1}{s} \qquad (2.29)$$

where A and B are arbitrary constants of integration and I_o and K_o are modified Bessels functions of 1st and 2nd kind respectively and of zeroth order. As

$$\bar{r} \to 0,\quad K_o(\sqrt{s}\ \bar{r}) \to \infty \qquad (2.30)$$

While physically, temperature of the component cannot be infinite, therefore, constant B should be zero and solution reduces to

$$\bar{\theta}(\bar{r},s) = \frac{1}{s} + A\,I_o(\bar{r}\sqrt{s}) \qquad (2.31)$$

Value of A can be calculated from boundary condition (2.25b). Therefore,

$$\bar{\theta}(\bar{r}, s) = \frac{1}{s} - \frac{\bar{q}\{\bar{\theta}(1,s)\}R}{K} \frac{I_o(\bar{r}\sqrt{s})}{\sqrt{s}\,I_1(\sqrt{s})} \qquad (2.32)$$

Using Appendix II and convolution theorem

$$\theta(\bar{r},Fo) = 1 - \frac{R}{K}\int_o^{Fo}\left[2+2\sum_{n=1}^{\infty}\frac{J_o(\mu_n\bar{r})}{J_o(\mu_n)}\exp\{-\mu_n^2(F_o-\tau)\}\right] q\{\theta(1,\tau)\}\,d\tau \qquad (2.33)$$

or

$$\theta(\bar{r},Fo) = 1 - Bi_{ref}\int_o^{Fo}\left[2+2\sum_{n=1}^{\infty}\frac{J_o(\mu_n\bar{r})}{J_o(\mu_n)}\exp\{-\mu_n^2(Fo-\tau)\}\right] \bar{h}\{\theta(1,\tau)\}\,\theta(1,\tau)\,d\tau \qquad (2.34)$$

where μ_n are roots of characteristic equation

$$J_0'(\mu) = J_1(\mu) = 0 \qquad (2.35)$$

Solution eqn.(2.34) also is a nonlinear, singular Volterra integral equation and for surface reduces to

$$\theta(1,Fo) = 1 - Bi_{ref} \int_0^{Fo} [2+2 \sum_{n=1}^{\infty} \exp\{-\mu_n^2 (Fo-\tau)\}]$$

$$\bar{h}\{\theta(1,\tau)\}\theta(1,\tau)d\tau \qquad (2.36)$$

Eqns. (2.21) and (2.36) can be written in a combined form

$$\theta(1, Fo) = 1 - Bi_{ref} \int_0^{Fo} [\beta_o + \sum_{n=1}^{\infty} \beta_n \exp\{-\mu_n^2 (Fo-\tau)\}]$$

$$\bar{h}\{\theta(1,\tau)\}\theta(1, \tau)d\tau \qquad (2.37)$$

where β_o and β_n are constants and μ_n are eigenvalues. Values for β_o, β_n and μ_n are given in Table 1 for three simple geometries.

Nonlinearity of eqn.(2.37) does not allow any closed form solution. Hence, we resort to numerical methods to solve this equation. Numerical methods have been discussed in the next chapter.

Table 1

S.No.	Geometry	β_o	β_k	λ_k	M_o	M_1
1.	Infinite Plate	1	2	k	1/3	1/45
2.	Infinite Cylinder	2	2	$J_1(\lambda_k)=0$	1/4	1/96
3.	Sphere	3	2	$\tan \lambda_k = \lambda_k$	1/5	1/175

CHAPTER 3

NUMERICAL TECHNIQUES

It was observed in the last chapter that the Volterra integral eqns. (2.20) and (2.34) were singular and nonlinear. Two different numerical methods for solving equations of this type have been suggested by Crosbie and Viskanta (1968a) and Crosbie and Banerjee (1973). These methods are discussed here.

3.1 SUCCESSIVE APPROXIMATION METHOD

This method was suggested by Crosbie and Viskanta (1968a). The nonlinearity in eqn. (2.20) arises due to nonlinearity of the boundary condition (2.6b) at the surface. For the surface eqn.(2.20), reduces to

$$\theta(1,Fo) = 1-Bi_{ref} \int_0^{Fo} [1+2 \sum_{n=1}^{\infty} \exp\{-n^2\pi^2(Fo-\tau)\}] \bar{h}\{\theta(1,\tau)\}\theta(1,\tau)d\tau \qquad (3.1)$$

Once eqn.(3.1) is solved for a dimensionless time τ, such that $0 < \tau < Fo$, then eqn.(2.20) can be solved for any coordinate $\bar{x}$ and time τ, because $\theta(1,\tau)$ and hence each term on right hand side of eqn.(2.20) will be known. The above equation can be solved by successive approximation method. An initial approximation is made for $\theta(1,\tau)$ and then it is improved by successive iteration. (k+1)th approximation can be given as

$$\theta(1,Fo)_{k+1} = 1-Bi_{ref} \int_0^{Fo} [1+2 \sum_{n=1}^{\infty} \exp\{-n^2\pi^2(Fo-\tau)\}]$$

$$\bar{h}\{\theta(1,\tau)_k\}\theta(1,\tau)_k \, d\tau \qquad (3.2)$$

For numerical solution, time period $0 < \tau < Fo$ is divided into m small intervals, such that

$$0 < t_1 < t_2 < t_3 < \ldots < t_{m-1} < Fo \qquad (3.3)$$

Then for the first interval $0 < \tau < t_1$, eqn.(3.2) can be rewritten as

$$\theta(1, t_1)_{k+1} = 1 - Bi_{ref} \int_0^{t_1} \left[1 + 2 \sum_{n=1}^{\infty} \exp\{-n^2 \pi^2 (t_1 - \tau)\} \right] \bar{h}\{\theta(1, \tau)_k\}\, \theta(1, \tau)_k \, d\tau \qquad (3.4)$$

This equation can be solved directly by successive approximation method. For second interval, $0 < \tau < t_2$, integral of eqn.(3.2), can be broken into two parts

$$\theta(1,t_2)_{k+1} = 1 - Bi_{ref} \int_0^{t_1} \left[1 + 2 \sum_{n=1}^{\infty} \exp\{-n^2 \pi^2 (t_2 - \tau)\} \right] \bar{h}\{\theta(1, \tau)\}\, \theta(1, \tau)\, d\tau$$

$$- Bi_{ref} \int_{t_1}^{t_2} \left[1 + 2 \sum_{n=1}^{\infty} \exp\{-n^2 \pi^2 (t_2 - \tau)\} \right] \bar{h}\{\theta(1, \tau)_k\}\, \theta(1, \tau)_k \, d\tau \qquad (3.5)$$

For first integral of equation (3.5), function $\theta(1,\tau)$ is known over a period of $0 < \tau < t_1$ from previous calculations. Hence eqn.(3.5), can be solved by assuming an initial approximation for $\theta(1, \tau)$ in the time interval $t_1 < \tau < t_2$ and improving it by iteration. Similarly (k+1)th approximation for mth interval is given by

$$\theta(1,Fo)_{k+1} = 1 - Bi_{ref} \int_0^{t_{m-1}} \left[1 + 2 \sum_{n=1}^{\infty} \exp\{-n^2 \pi^2 (Fo - \tau)\} \right] \bar{h}\{\theta(1, \tau)\}\, \theta(1,\tau)\, d\tau$$

$$- Bi_{ref} \int_{t_{m-1}}^{Fo} \left[1 + 2 \sum_{n=1}^{\infty} \exp\{-n^2 \pi^2 (Fo - \tau)\} \right] \bar{h}\{\theta(1, \tau)_k\}\, \theta(1,\tau)_k \, d\tau \qquad (3.6)$$

The choice for initial approximation is of great importance. Convergence will be faster if initial approximation is closer to exact solution. This will save computation time. Crosbie and Viskanta (1968a) used the solution of the following equation as an initial approximation.

$$\theta(1,Fo) = 1-Bi_{ref}\int_{o}^{t_{m-1}}\left[1+2\sum_{n=1}^{\infty}\exp\{-n^2\pi^2(Fo-\tau)\}\right]\bar{h}\{\theta(1,\tau)\}\theta(1,\tau)\,d\tau$$

$$-Bi_{ref}\,\bar{h}\{\theta(1-Fo)\}\,\theta(1,Fo)\int_{t_{m-1}}^{Fo}\left[1+2\sum_{n=1}^{\infty}\exp\{-n^2\pi^2(Fo-\tau)\}\right]d\tau \qquad (3.7)$$

The above equation can be solved for $\theta(1,Fo)$ as terms contained in the both integrals are only known terms and hence integrals can be evaluated. It can be seen that eqn.(3.7), represents a first order approximation to eqn.(3.6), by neglecting the variation of $\bar{h}\{\theta(1,\tau)\}\theta(1,\tau)$ in the time interval t_{m-1} to Fo. On the other hand, when time interval t_{m-1} to Fo is small, value of $\theta(1,t_{m-1})$ can be used as an initial approximation for $\theta(1,Fo)$. This is being used in the present work. The kernels of integrals in eqns. (3.4), (3.5) and (3.6) are singular because infinite series does not converge at $\tau = Fo$ and summation of infinite series tends to infinity. This singularity of kernel can be removed by Poission summation formula (see Appendix III)

$$1+2\sum_{n=1}^{\infty}\exp\{-n^2\pi^2(Fo-\tau)\} = \left[1+2\sum_{n=1}^{\infty}\exp\{-n^2/(Fo-\tau)\}\right]\{\pi(Fo-\tau)\}^{-\frac{1}{2}} \qquad (3.8)$$

and after substituting it in eqn.(3.6), integral is evaluated by the use of of modified Gaussian integration formula, Devis and Polonsky (1965), which states

$$\int_{t_{m-1}}^{Fo} f(\tau)(Fo-\tau)^{-\frac{1}{2}}\,d\tau = 2(Fo-t_{m-1})^{\frac{1}{2}} \sum_{i=1}^{N} w_i^{(2N)} f(\tau_i) \quad (3.9)$$

where

$$\tau_i = t_{m-1} + (Fo-t_{m-1})(1-x_i^2)$$

and $w_i^{(2N)}$ = Gaussian weightage of order (2N).

Substituting eqn.(3.9), in eqn.(3.6), we get

$$\theta(1,Fo) = 1-Bi_{ref} \int_{o}^{t_{m-1}} [\,1+2\sum_{n=1}^{\infty} \exp\{-n^2\pi^2(Fo-\tau)\}]\,\bar{h}\{\theta(1,\tau)\}\theta(1,\tau)\,d\tau$$

$$- 2Bi_{ref}(\Delta t/\pi)^{\frac{1}{2}} \sum_{i=1}^{N} w_i^{(2N)}[\,1+2\sum_{n=1}^{\infty} \exp\{-n^2/(\Delta t\, x_i^2)\}]\,\bar{h}\{\theta(1,\tau_i)\}\theta(1,\tau_i) \quad (3.10)$$

where $\Delta t = Fo-t_{m-1}$.

3.2 SEPARABLE KERNEL METHOD

A method which is simpler than the successive approximation method was also suggested by Crosbie and Viskanta (1968b). This method is known as the 'Separable Kernel Method'. The kernel in the integral eqn.(2.37) is represented by an infinite series. In the separable kernel method,the infinite series is truncated at a suitable point, i.e. symbolically, the kernel of eqn. (2.37)

$$f = \beta_o + \sum_{n=1}^{\infty} \beta_n \exp\{-\mu_n^2(Fo-\tau)\} \quad (3.11)$$

is approximated by a separable kernel

$$fa = \beta_o + \sum_{n=1}^{M} \beta_n \exp\{ -\mu_n^2(Fo-\tau) \} \qquad (3.12)$$

Later this kernel was modified by Crosbie and Banerjee (1973), for taking into account the other terms of infinite series. Modified kernel is

$$fa = \beta_o + \sum_{n=1}^{M-1} \beta_n \exp\{ -\mu_n^2(Fo-\tau)\} + \varepsilon_M \beta_M \exp\{-b_M(Fo-\tau)\} \qquad (3.13)$$

Then the nonlinear singular Volterra integral eqn.(2.37), can be written as

$$\theta(1,Fo) = 1 - Bi_{ref}\beta_o \int_o^{Fo} \bar{h}\{\theta(1,\tau)\}\theta(1,\tau)d\tau$$

$$- \sum_{n=1}^{M-1} Bi_{ref}\,\beta_n \int_o^{Fo} \exp\{-\mu_n^2(Fo-\tau)\}$$

$$\bar{h}\{\theta(1,\tau)\}\,\theta(1,\tau)d\tau$$

$$- Bi_{ref}\,\varepsilon_M\beta_M \int_o^{Fo} \exp\{-b_M(Fo-\tau)\}\bar{h}\{\theta(1,\tau)\}\,\theta(1,\tau)d\tau \qquad (3.14)$$

and solution to the above equation can be split into (M+1) parts

$$\theta(1,Fo) = \theta_o(1,Fo) + \theta_1(1,Fo) + \ldots + \theta_M(1,Fo) \qquad (3.15)$$

where

$$\theta_o(1,Fo) = 1 - Bi_{ref}\,\beta_o \int_o^{Fo} \bar{h}\{\theta(1,\tau)\}\theta(1,\tau)d\tau \qquad (3.16a)$$

$$\theta_1(1,Fo) = -Bi_{ref}\,\beta_1 \int_o^{Fo} \exp\{-\mu_1^2(Fo-\tau)\}$$

$$\bar{h}\{\theta(1,\tau)\}\theta(1,\tau)d\tau \qquad (3.16b)$$

$$\theta_{M-1}(1,Fo) = -Bi_{ref} \beta_{M-1} \int_{o}^{Fo} \exp\{-\mu_{M-1}^{2}(Fo-\tau)\}$$

$$\bar{h}\{\theta(1,\tau)\}\ \theta(1,\tau)d\tau \qquad (3.16c)$$

and (M+1)th term can be written as

$$\theta_{M}(1,Fo) = -Bi_{ref} \varepsilon_{M} \beta_{M} \int_{o}^{Fo} \exp\{-b_{M}(Fo-\tau)\}$$

$$\bar{h}\{\theta(1,\tau)\}\ \theta(1,\tau)d\tau \qquad (3.16d)$$

Differentiating above equations with respect to Fo once, we will get (M+1) simultaneous differential equations connected by eqn.(3.15). The set of differential equation is given as

$$\frac{d\theta_{o}(1,Fo)}{dFo} = 1 - \beta_{o}\, Bi_{ref}\, \bar{h}\{\theta(1,Fo)\}\theta(1,Fo) \qquad (3.17a)$$

$$\frac{d\theta_{1}(1,Fo)}{dFo} = -\beta_{1}\, Bi_{ref}\, \bar{h}\{\theta(1,Fo)\}\theta(1,Fo) - \mu_{1}^{2}\theta_{1}(1,Fo) \qquad (3.17b)$$

$$\frac{d\theta_{M-1}(1,Fo)}{dFo} = -\beta_{M-1}\, Bi_{ref}\, \bar{h}\{\theta(1,Fo)\}\theta(1,Fo) - \mu_{M}^{2}\theta_{M-1}(1,Fo) \qquad (3.17c)$$

and

$$\frac{d\theta_{M}(1,Fo)}{dFo} = -\varepsilon_{M}\beta_{M}\, Bi_{ref}\, \bar{h}\{\theta(1,Fo)\}\theta(1,Fo) - b_{M}\theta_{M}(1,Fo) \qquad (3.17d)$$

As these are (M+1) first order differential equations (3.17), (M+1) initial conditions are also needed. These are obtained from eqns(3.16) by setting Fo = 0.

$$\theta_o(1,0) = 1 \qquad (3.18a)$$

$$\theta_1(1,0) = \theta_2(1,0) = \theta_M(1,0) = 0 \qquad (3.18b)$$

and which on substitution into eqn.(3.15) becomes

$$\theta(1,0) = 1 \qquad (3.19)$$

Values of factors ε_M and b_M in eqn. (3.17d), may be calculated using following two properties of the kernel

$$M_o = \int_o^\infty [\, f - \beta_o] \, dFo = \sum_{n=1}^{\infty} (\beta_n / \mu_n^2) \qquad (3.20)$$

$$M_1 = \int_o^\infty [f - \beta_o] Fo \; dFo = \sum_{n=1}^{\infty} (\beta_n / \mu_n^4) \qquad (3.21)$$

Values of M_o and M_1 are given in Table 1.

One way to find out the values of ε_M and b_M is as follows:

$$\text{assume } b_M = \mu_M^2 \qquad (3.22)$$

Then

$$\int_o^\infty [\, fa - \beta_o] dFo = \sum_{n=1}^{M-1} \frac{\beta_n}{\mu_n^2} + \frac{\varepsilon_M \beta_M}{\mu_M^2}$$

$$= M_o \qquad (3.23)$$

Therefore,

$$\varepsilon_M = \mu_M^2 (M_o - \sum_{n=1}^{M-1} \frac{\beta_n}{\mu_n^2}) / \beta_M \qquad (3.24)$$

and last differential equation (3.17d) changes to

$$\frac{d\theta_m(1,Fo)}{dF_o} = - \varepsilon_M \beta_M \, Bi_{ref} \, \bar{h}\{\theta(1,Fo)\} \theta(1,Fo) - \mu_M^2 \, \theta_M(1,Fo) \qquad (3.25)$$

Then these simultaneous differential equation can be solved by any standard method. In the present study Runge-Kutta fourth order formula is used for solving these differential equations.

3.3 NUMERICAL DIFFICULTIES AND THEIR REMEDIES

3.3.1 SUMMATION OF INFINITE SERIES:

Kernel of integral eqn.(2.20) is a convergent infinite series. Series contains two factors, oscillating at different frequencies and their superimposed frequency is different from both. The factors are $(-1)^n$ and $\cos n \pi x$.

For the numerical summation, above series has to be truncated at a suitable point such that terms after than point can be neglected in comparison to sum of the series. If this criteria is based on a comparison of single term, after the truncation point, with sum of the series, results will be in error. The error arises because any single term may be small in comparison with the sum though the rest of the truncated terms may not be negligible. The other reason is, individual terms may be large enough, but the algebraic sum may be small because of oscillating nature of series. Hence the criteria for truncation should be based on a comparison of sum of a complete cycle with sum of the series.

3.3.2 CHOICE OF TIME STEP IN EQN.(3.10):

A good plot between temperature and time is required for analysing a quench hardening. For a close to exact solution and smooth curve, temperature must be known after each small time interval (Δ t in eqn.3.10). Choice of this time interval is very critical.

It depends upon the maximum Biot number. Too small a time interval will lead to a very large computation time while a large time interval will lead to a divergence in the numerical scheme.

Observing eqn.(3.10) for m=1, equation gives a relation for $\theta(1,Fo)$ as

$$1-\theta(1,Fo) \propto Bi_{ref}\ \bar{h}\{\theta(1,\tau)\}\theta(1,\tau)\ (\Delta t)^{\frac{1}{2}} \qquad (3.26)$$

This relation can be reduced to

$$\Delta t \sim \frac{c_1}{\left[Bi_{ref}\ \bar{h}\{\theta(1,\tau)\}\theta(1,\tau)\right]^2} \qquad (3.27)$$

where c_1 is a constant of proportionality. Value of c_1 is found by comparing results for different values of Biot number and time step, Δt, with Heisler charts. This enables to make an optimum choice of Δt as

$$\Delta t = \frac{0.01}{\left[Bi_{ref}\ \bar{h}\{\theta(1,\tau)\}\theta(1,\tau)\right]^2} \qquad (3.28)$$

3.4.1 EXPERIMENTAL SET-UP:

Some experiment were also performed to verify the numerical results for cylinder and plate. A set up was made consisting of a furnace, a water reservoir, a recording unit and a transporting mechanism. The transporting mechanism was an assembly of a drum and a platform which could move on a pair of rails.(see photograph on page 31).

The component can be held in any position with the help of a wire rope wraped on the drum. The recording unit was an Encardio-Rite four-channel recorder. It is made of the differential amplifiers

for amplifying the thermocouple output, the galvano meter for deflecting the needle and the chart drive motor with a variable speed gear set.

The component which made of mild steel was heated in the furnace at a constant temperature for a sufficiently long time to ensure the uniform temperature. The heated component was quenched by suspendong it in the middle of water reservoir which was the quenching medium. The temperatures were recorded with the help of thermocouples embedded at center and at the surface. For ensuring the proper contact at the center, an arrangement was used as shown in Fig.4. A chart speed of 1 mm/sec. was used for recording the temperature.

The thermocouple used was Alumel-Chromel of gage 24 B&S insulated with Teflon. ISA code for these are KN and KP. These can measure a temperature upto 280°C with an error of $\pm 2\%$ and upto 1260°C with an error of $\pm 0.6\%$.

3.4.2 EXPERIMENTAL DIFFICULTIES:

The main problem faced was to shield the thermocouple from water. For this purpose the Sauereisen insolute adhesive cement was used but this cement desolves in the water. Hence, a layer of Aral-dite was coated on the cement which can withstand temperatures of the order of 200°C (used in the experiments). For the higher temperature, one has to look for a better coating.

The results obtained by numerical method and experiments are compared in the next chapter.

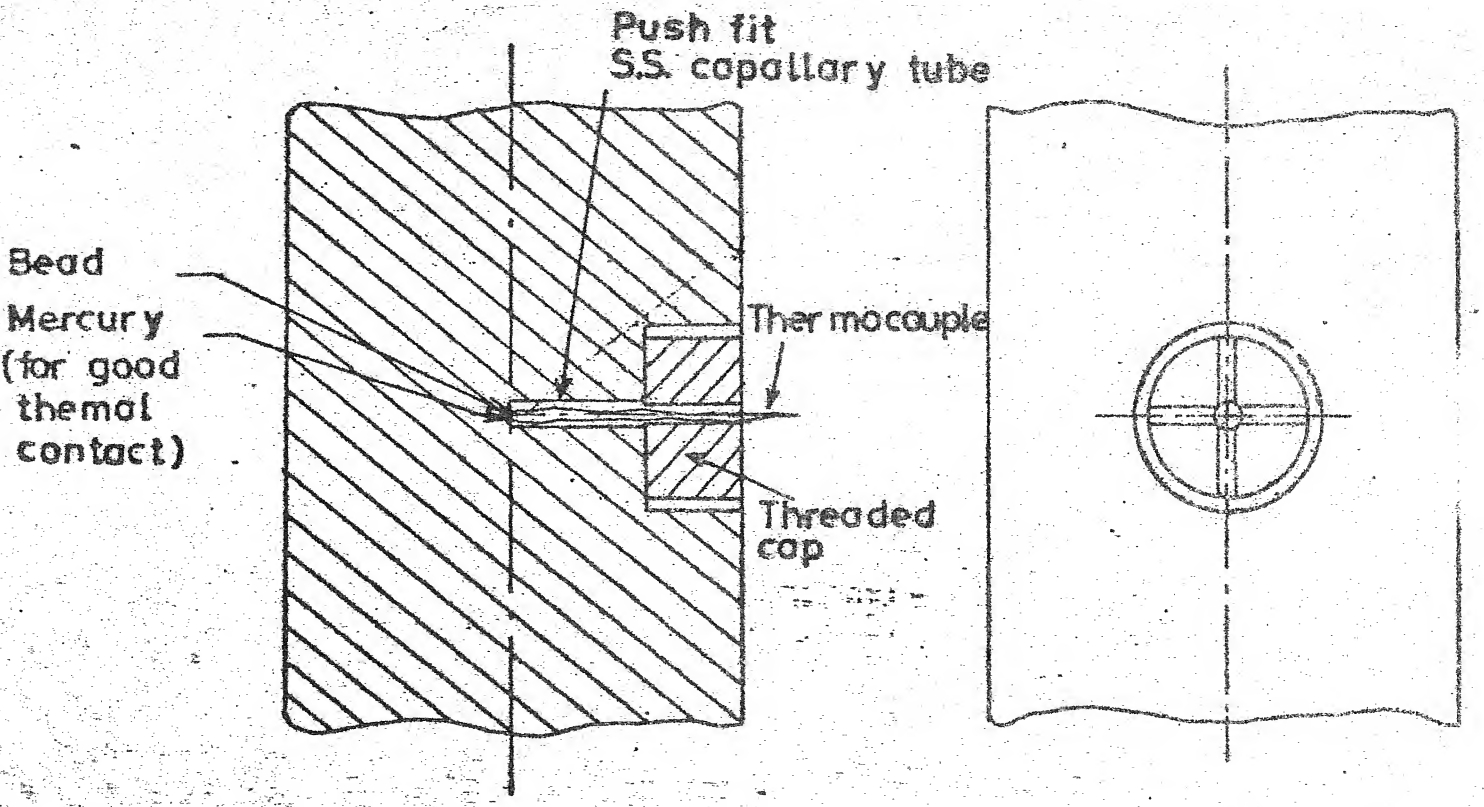

Fig. 4 Arrangement for fixing the thermocouple at the centre

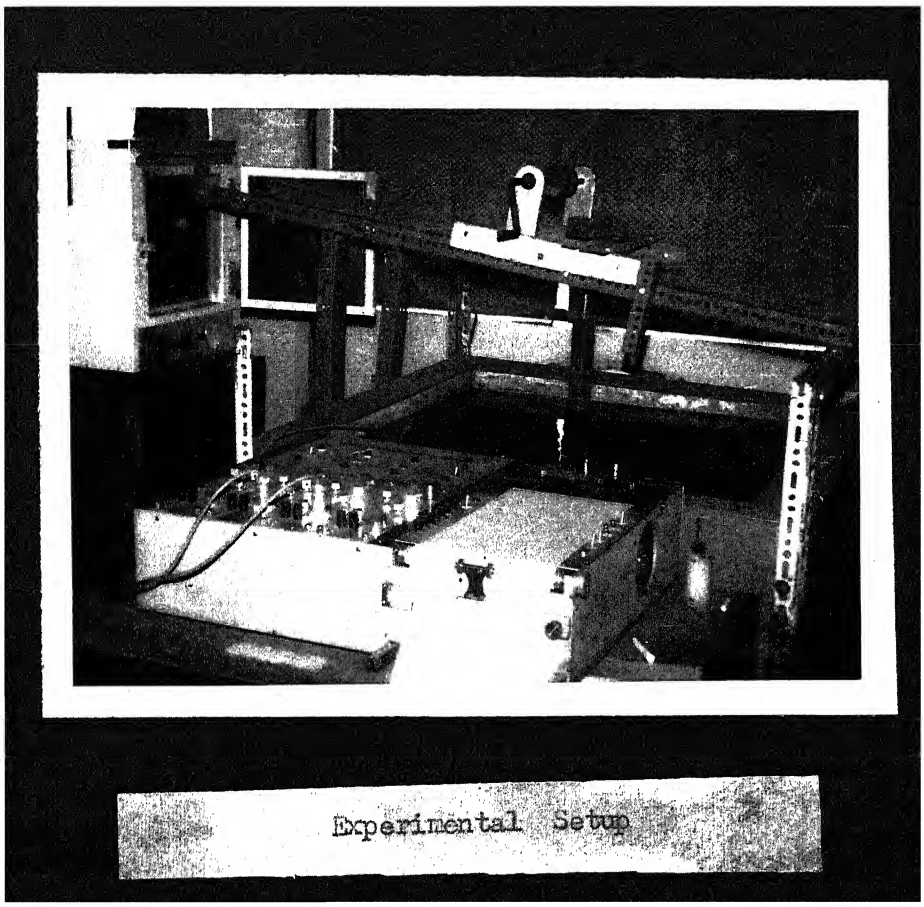

Experimental Setup

CHAPTER 4

RESULTS AND DISCUSSION

Solution obtained using numerical methods discussed in last chapter are presented here. First the numerical methods are compared with standard results available from Heisler's charts. This comparision will give some idea of the accuracy of the methods. Then these results are compared with the results available in literature and those obtained by experiments.

In Table 2, the results of successive iteration method for the case of constant heat transfer coefficient (and various values of time steps) are compared with results of Heisler (1947) for various values of Biot number. It can be seen from Table 2 that for Biot nos. of 2,10,200, the optimum time step for which the agreement with Heisler's results are best are 0.01, 0.0004 and 0.000001 respectively. These results are in agreement with the dependence of time step on Biot number assumed in eqn. (3.27) and the value of C_1 is seen to be 0.01.

In Fig.5, the results of successive iterative method for different Biot number are compared with Heisler's results. The results are in perfect agreement for low Biot number but becomes progressively worse as Biot number increases. It is also observed that error increases at large Fourier number. This can be inferred from equation (3.7). The infinite series in equation (3.7) converges very slowly for small Fourier numbers. Any error in the evaluation of

Table 2

Bi = 2

Fo	Heisler's results	Time step		
		0.005	0.01	0.05
0.1	0.55354	0.55393	0.55355	0.54485
0.2	0.45759	0.45792	0.45770	0.45411
0.3	0.35231	0.35248	0.35237	0.35066
0.4	0.22091	0.22090	0.22083	0.21969
0.9	0.19672	0.19669	0.19662	-

Bi = 10

Fo	Heisler's results	Time step		
		0.0001	0.0004	0.001
0.04	0.25928	0.26493	0.26469	0.5477
0.08	0.19467	0.20232	0.20214	0.18543
0.12	0.16054	0.17149	0.17136	0.14828
0.16	0.13837	0.14973	0.14961	0.12609
0.20	0.12429	0.13653	0.13642	0.11096

Bi = 200

Fo	Heisler's results	Time step		
		0.5×10^{-6}	10^{-6}	10^{-5}
0.0004	0.26153	0.27746	0.27491	0.25013
0.0008	0.19192	0.21128	0.20887	0.17352
0.0012	0.15441	0.17578	0.17353	0.13447
0.0016	0.12876	0.15386	0.15145	0.10381
0.0020	0.11349	0.13903	0.13823	-

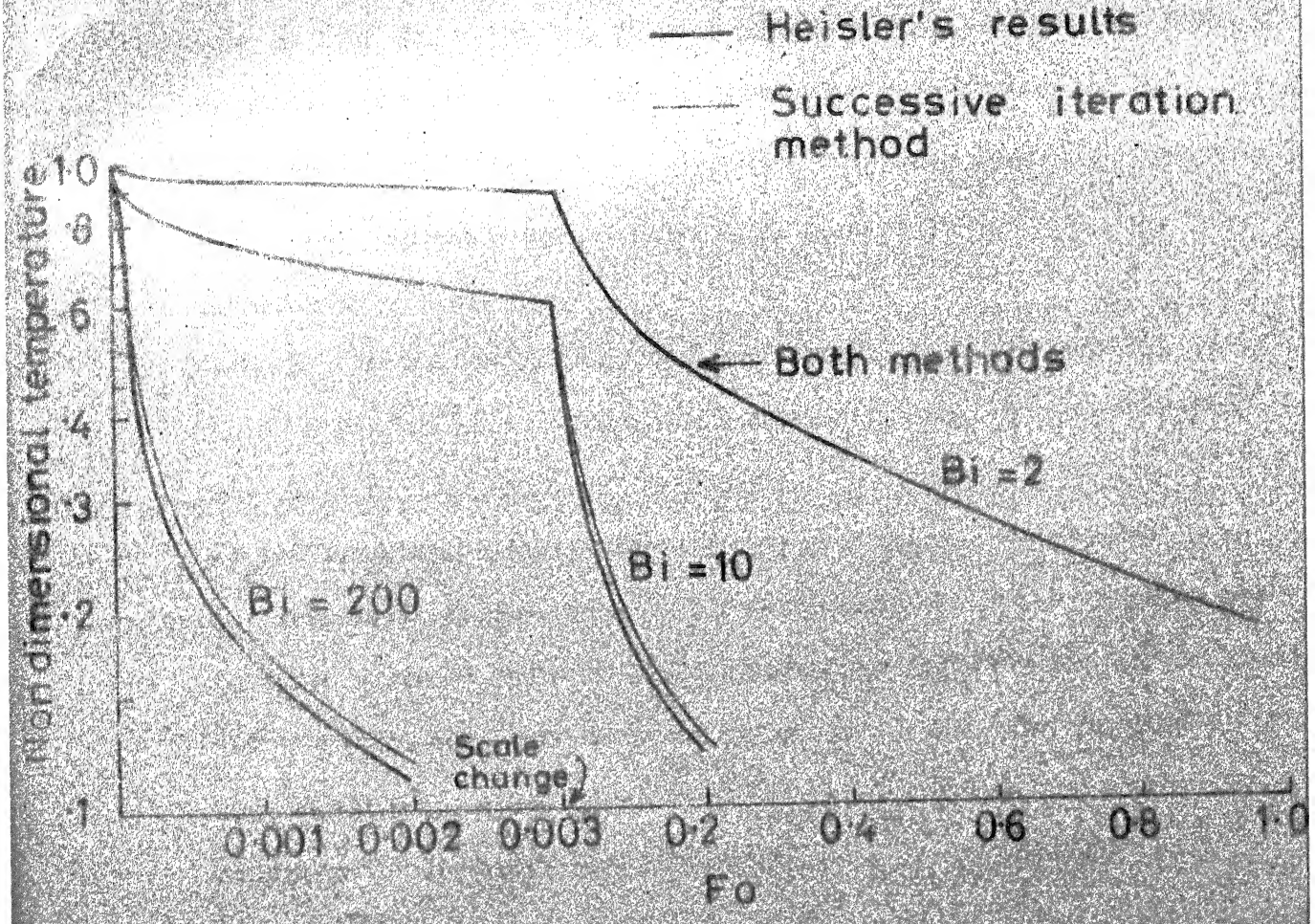

Fig. 5 Comparision between successive iteration method and Heisler's results for plate surface

the sum of the infinite series is amplified at large Biot numbers. Hence this method will lead to significant errors at high Biot numbers and low Fourier numbers. Note that at high Biot numbers, the cooling rate is high and hence the Fourier number of interest will necessarily be small. The error increases as time increases because of the accumulation of error.

The separable kernel method is first validated for constant heat transfer coefficient by comparing it with results presented by Heisler (1947). In Fig.6, it is observed that the agreement is again perfect for low Biot no. but results deviate more and more from the Heisler's results for high Biot number. It is also observed that separable kernel method initially overpredicts the temperature but after a particular time it tends to underpredict. The maximum error in temperature is found to be at low fourier numbers where it is about 16%. But, if the error is based on the prediction time to reach a particular temperature (i.e. $\frac{\text{Time}_{SKM} - \text{Time}_{Heisler}}{\text{Time}_{Heisler}}$), the error is considerably lower (of the order of 5%).

In Fig.7, the effect of the number of simultaneous differential equations (3.17) used on the accuracy of separable kernel method is seen. It is observed that as the number of equations are increased separable kernel method predicts the values approaching the Heisler's. It implies that more terms should be considered in the infinite series for high Biot number such that the last term of the kernel, $\exp(-\mu_n^2 f_o)$ becomes negligible.

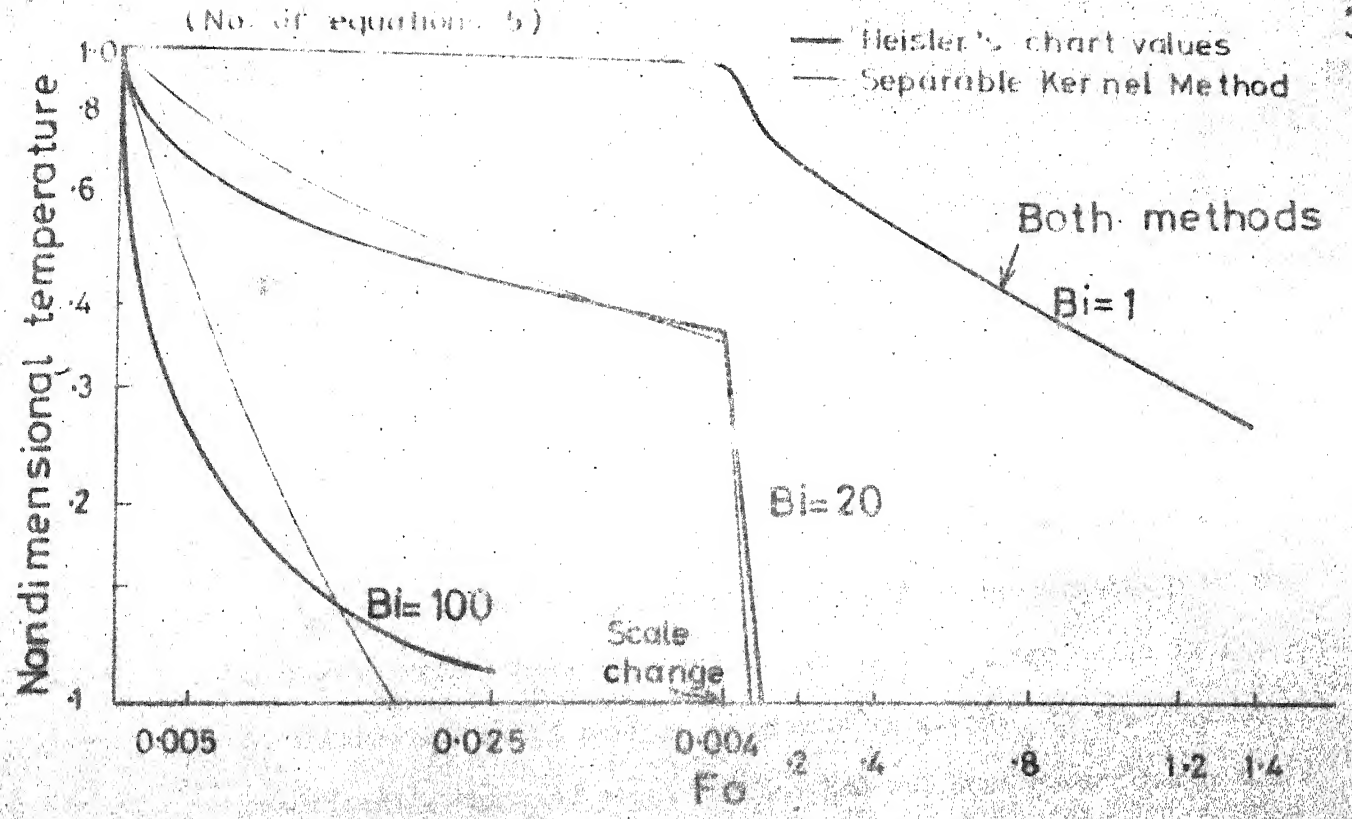

Fig. 6 Comparision between "Separable Kernel Method" and Heisler's chart for plate surface

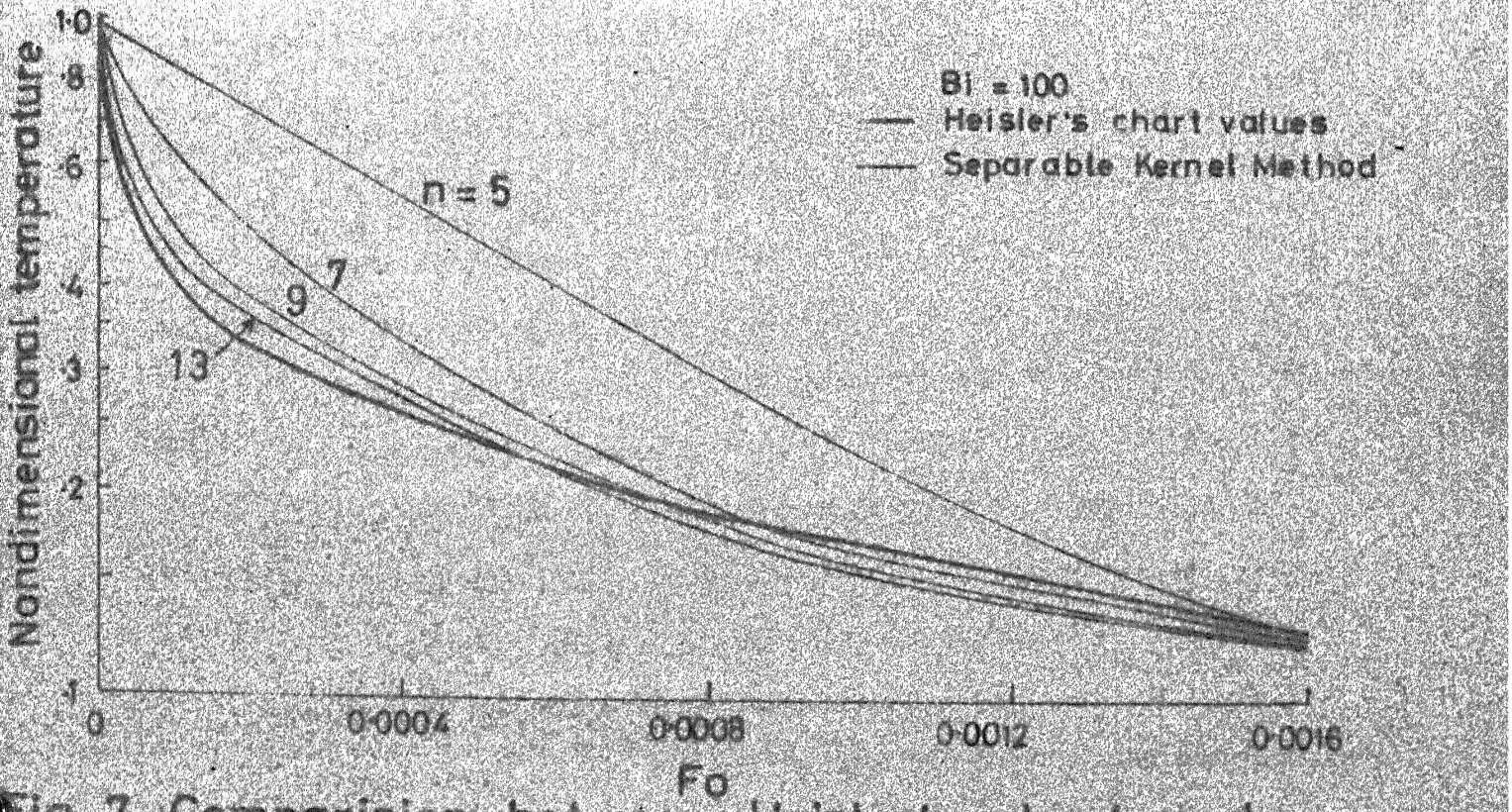

Fig. 7 Comparision between Heisler's chart and separable kernel method with various number of equations, for plate surface

In Fig.8, the results of successive iteration method for a plate for two different values of constant C_{sf} in eqn.(A4.5), are compared with the experimental observations. It is found that results for C_{sf}= 0.006 matches the experimental results better than that of C_{sf}= 0.013. This can also be seen in Fig.9 where the separable kernel method is compared with experimental results for two values of C_{sf} The value of C_{sf} depends strongly on the condition of the surface. Unfortunately, where the value of C_{sf} are given in literature no information about surface roughness is given. In the present experiments, the mild steel surface had not been ground hence the surface was quite rough. Therefore, it seems justifiable to use the low value of C_{sf} (which will result in higher boiling heat transfer coefficient, see eqn.(A4.5).

Successive iteration method may be called as exact method because ideally accuracy can be maintained by a proper choice of time step and more number of iterations. But, if it is not possible to avoid round-off error (because of limit on the number of significant digits that can be stored on the computer) then this method is not useful since the error tends to accumulate with time. On the other hand, in the separable kernel method the error in the previous step damps out rapidly. This is because the error in Runge-Kutta method, which is used in solution of simultaneous differential equations(3.17), decreases if the slope of the temperature - time curve decreases, (see Rajaraman (1974)). In addition the accuracy can be increased to any desired degree by simply increasing the number of equations. This is illustrated in Fig.10.

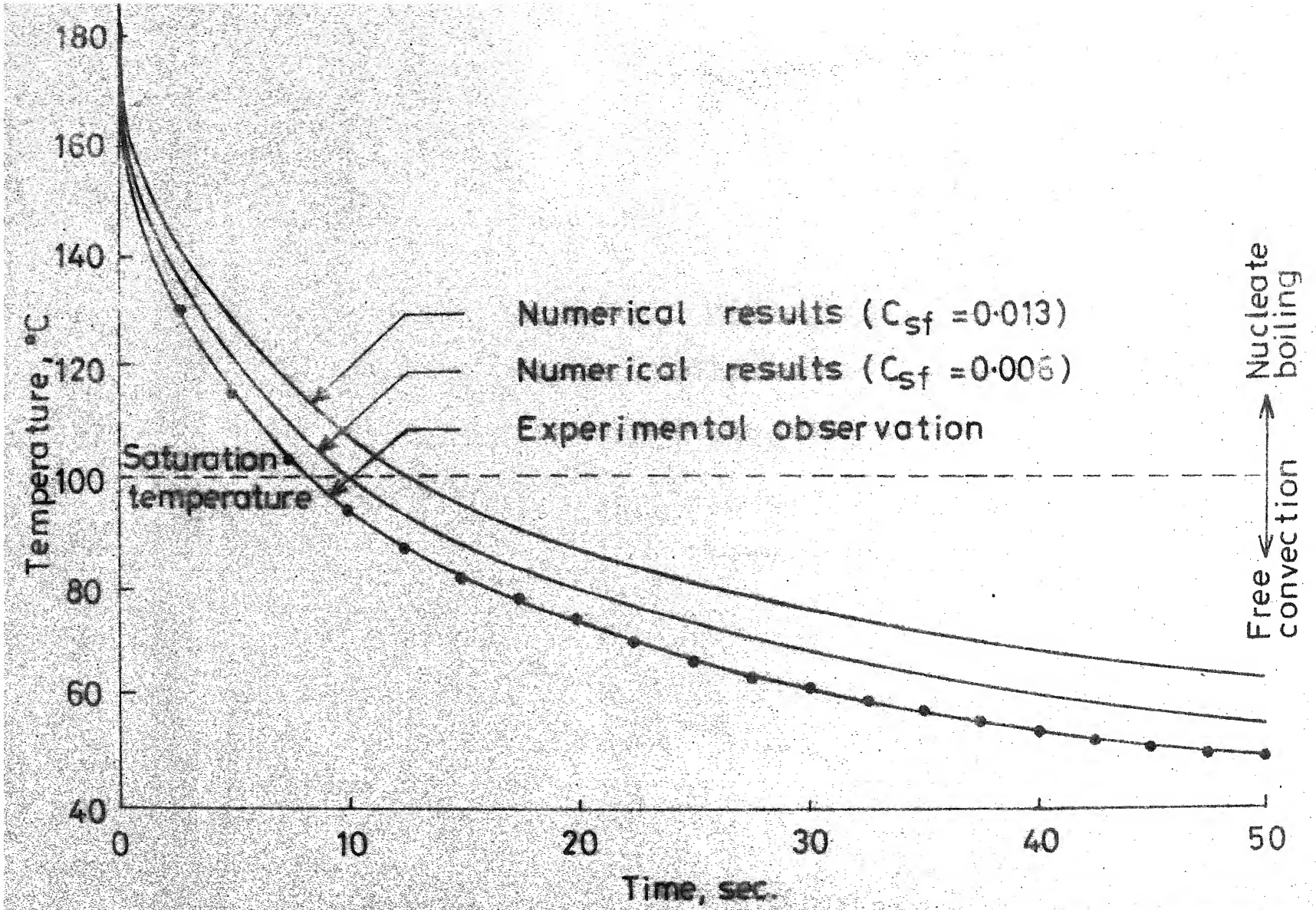

Fig. 8 Comparision between experiment and successive iteration method for two values of constant in corretation for nucleate boiling heat transfer, for plate surface

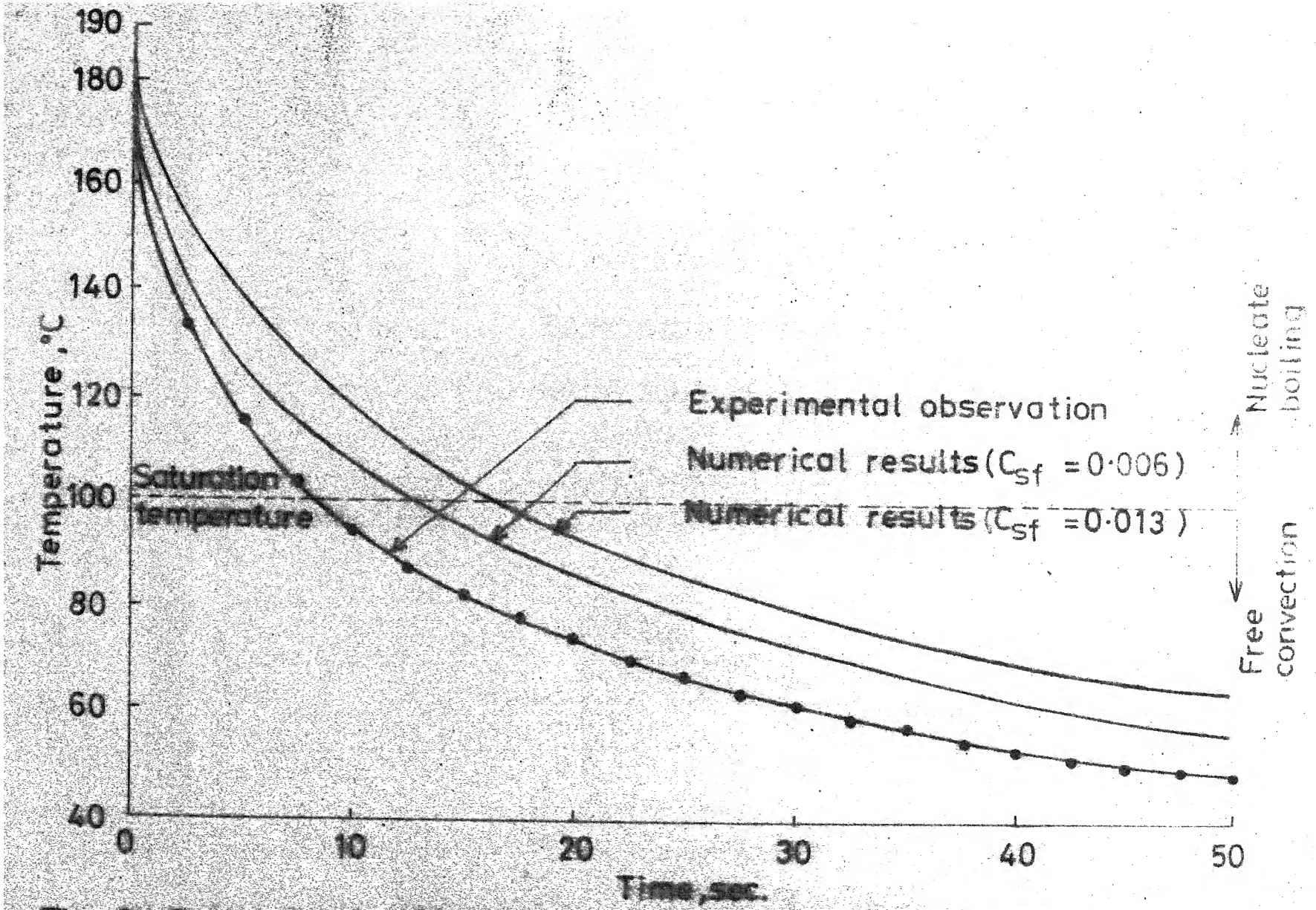

Fig. 9 Comparison between experiment and separable kernel method for two values of constant in correlation for nucleate boiling heat transfer, for plate surface

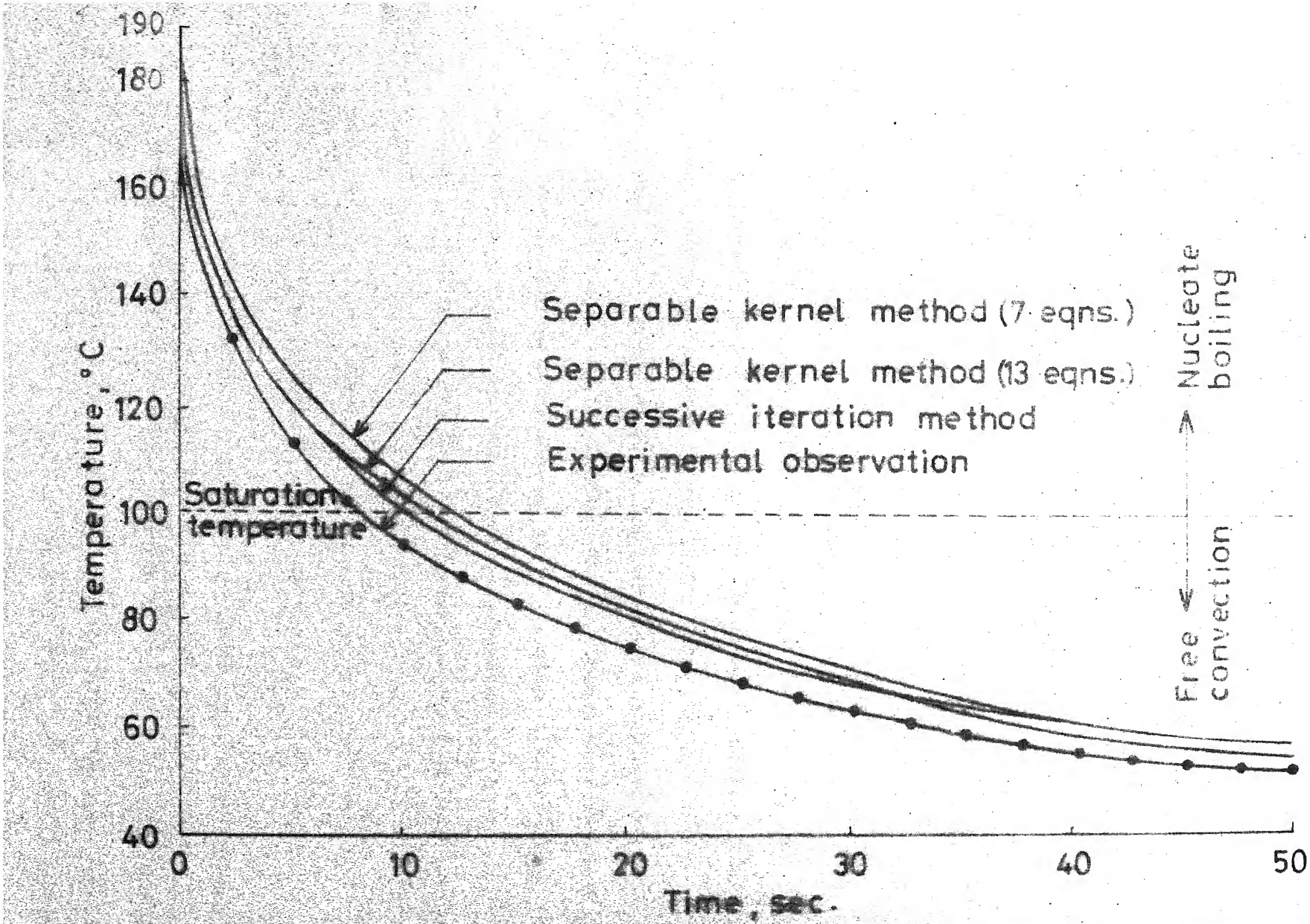

Fig. 10 Comparision between experiment, successive iteration method and separable kernel method with various number of equations, for plate surface

In Fig.11, experimental results for the temperature at the plate centre are compared with that of separable kernel method. It can be seen that numerical scheme shows a continuous fall in temperature from the very beginning, while experimental results show no fall for sometime. The variation of temperature at the centre is slower in the beginning and it looks as though the recording instrument is unable to sense it. At large fourier number error is much higher.*

Same trend is observed for cylinder surface and centre also (Figs. 12,13).

In the above presentation film boiling could not be illustrated. This was because of laboratory limitations, it was not possible to reach high temperature needed to achieve film boiling. However, experimental results for film boiling are available from Bofors Handbook (Thelning 1975) and these compared with the numerical solution in Figs. 14,15. Though the deviation is very large, trend is again same as in the previous illustrations. Temperature predicted is higher than the experimental results available. The reason may be an improper choice of correlations. Unfortunately, the conditions are not mentioned in the literature, also he mentioned that the cooling capacity of water is increased very considerably by adding 10% of common salt or soda to the water. With such a information, the over-prediction of temperature was expected.

* One reason for higher error may be thought as end losses due to limited size of specimen. But the error was, calculated by so called Newman method, very small because of the low Fourier number for the ends.

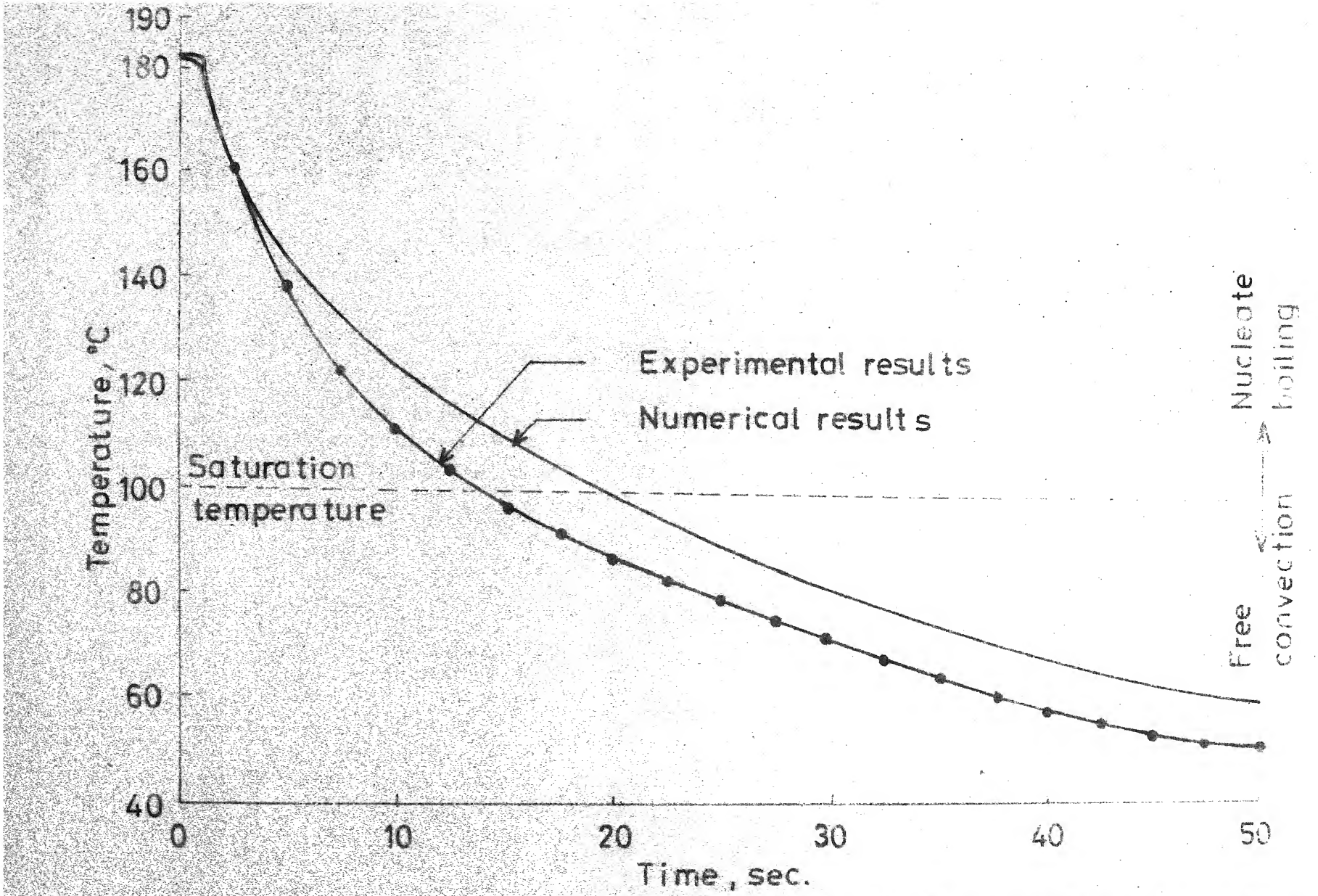

Fig.11 Comparison of the temperature at the centre of the plate obtained by experiment and separable kernel method

Fig.12 Comparison of the temperature at the surface of the cylinder obtained by experiment and separable kernel method

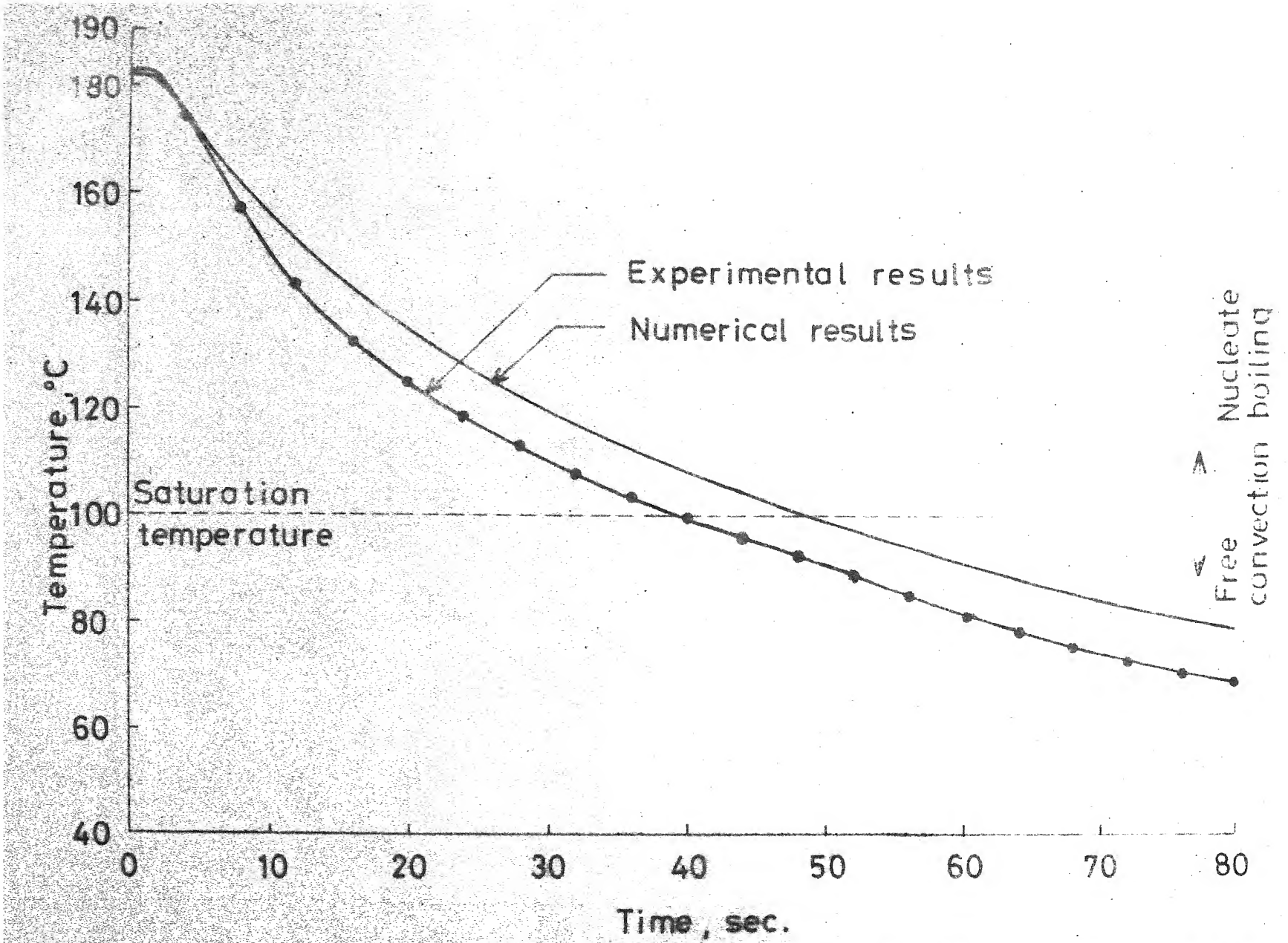

Fig. 13 Comparison of the temperature at the centre of the cylinder obtained by experiment and separable kernel method

Fig. 14 Comparision of the temperature at the surface of the cylinder avaiable in literature and separable kernel method

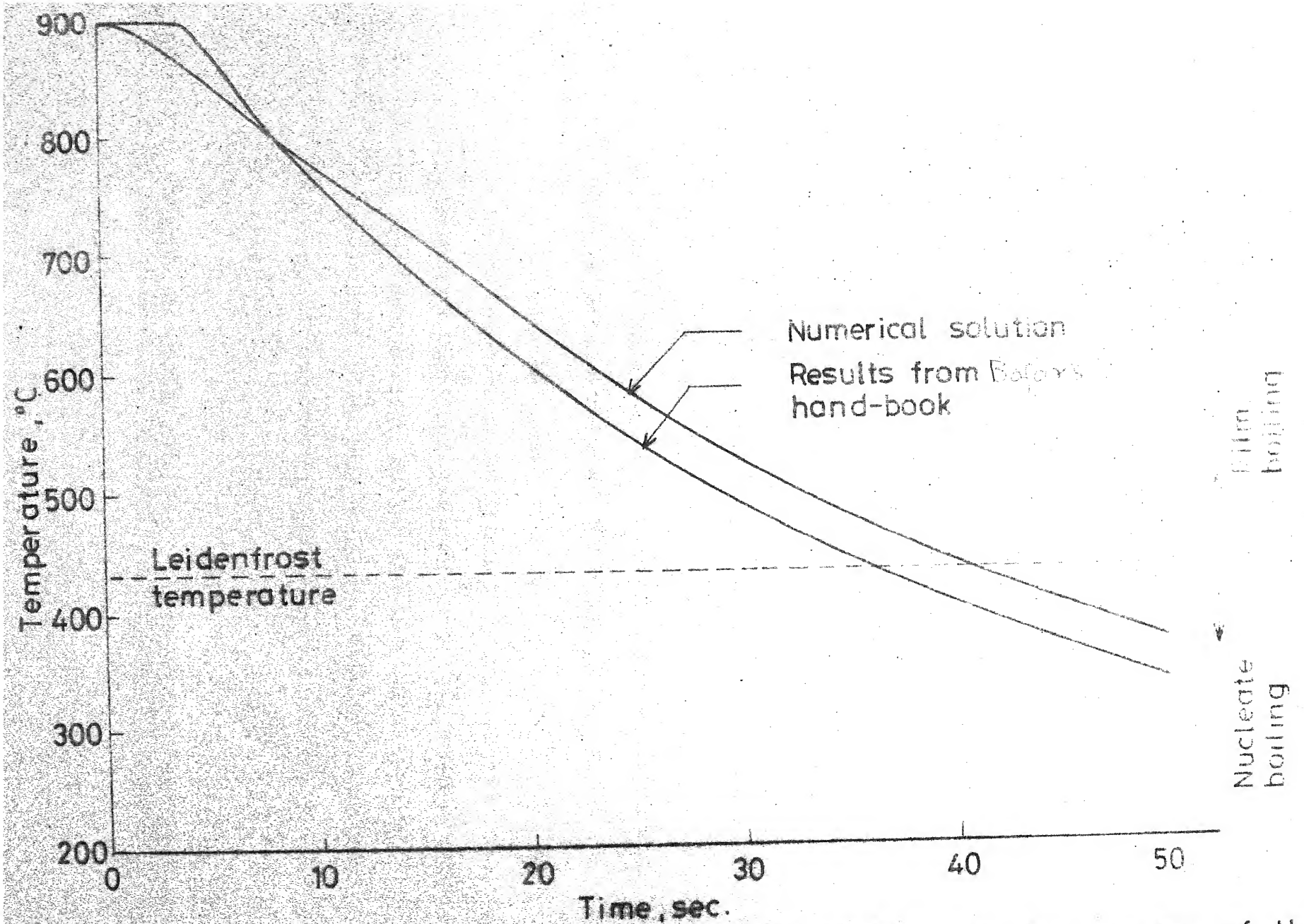

Fig. 15 Comparision of the temperature profile at the centre of the cylinder available in the literature and separable kernel method

CONCLUSION : The present work is not merely of theortical interest. In the industries, often we face an inverse problem, where one desires a component of specific alloy with specific qualities and suitable rate of cooling has to be found out. The present computing techniques will judge whether the choice of cooling system is proper. If it is not so, one may vary the cooling rate by using another quenchent or adding some chemicals to the same quenchent. Cooling rate may also be increased by mechanical vibration to the component in film boiling regim. This intermittently breaks the film layer.

We may control the depth of hardness also by choosing the proper cooling rate. From the figs. 10 and 11, we can see that, the cooling rate at centre is faster than at the surface. Hence, by increasing the cooling rate we can decrease the depth of hardness and vice-versa.

Keeping the dignosis of error in two methods in view, we may use the two methods simultaneously for more accurate results. The successive iteration method may be used for low fourier number, where one needs more accuracy, without much increasing computation time. But at the later stage, when successive iteration method begins to deviate due to accumulation of error, we may switch over to separable kernel method.

APPENDIX I

The following expressions are known as Theta functions.

$$\theta_3(\mu) = \theta_3(\mu/\tau) = \sum_{n=-\infty}^{\infty} \exp(i\pi\tau n^2)\exp(2n\mu i) \qquad (A1.1)$$

$$= 1 + 2\sum_{n=1}^{\infty}\exp(i\pi\tau n^2)\cos 2n\mu$$

and

$$\theta_4(\mu) = \theta_4(\mu/\tau) = \sum_{n=-\infty}^{\infty}(-1)^n \exp(i\pi\tau n^2)\cdot\exp(2n\mu i) \qquad (A1.2)$$

$$= 1+2\sum_{n=1}^{\infty}(-1)^n e^{i\pi\tau n^2}\cos 2n\mu$$

where $\exp(i\pi\tau) = q$ (A1.3)

and $|q| < 1$ (A1.4)

Hence, singular kernel of eqn.(2.20) is also a Theta function

$$1+2\sum_{n=1}^{\infty}(-1)^n\cos n\pi x \exp\{-n^2\pi^2(Fo-\tau)\}$$

$$= \theta_4\{\frac{\pi x}{2} / i\pi(Fo-\tau)\}$$

$$= \theta_3\{\frac{\pi(1-x)}{2} / i\pi(Fo-\tau)\} \qquad (A1.5)$$

Some relations are given by Gradshteyn and Ryzhik (1965), few of those are mentioned below.

$$\theta_4(\mu+\pi) = \theta_4(\mu) = \theta_4(-\mu) \qquad (A1.6)$$

$$\theta_3(\mu+\pi) = \theta_3(\mu) = \theta_3(-\mu) \qquad (A1.7)$$

$$\theta_4(\mu+\frac{\pi}{2}) = \theta_3(\mu) \qquad (A1.8)$$

$$\theta_3(\mu+\frac{\pi}{2}) = \theta_4(\mu) \qquad (A1.9)$$

APPENDIX II

INVERSE LAPLACE TRANSFORMATION BY SERIES EXPANSION

In this method of Inverse Laplace transformation, $F(s)$, the image function of $f(t)$ is expanded in a series,

$$F(s) = \sum_{n=0}^{\infty} F_n(s) \qquad (A2.1)$$

in which the terms $F_n(s)$ are image ~~xx~~functions of $f_n(t)$. Then solution is obtained by transforming this series term by term, Doetsch (1971)

$$f(t) = \sum_{n=0}^{\infty} f_n(t) \qquad (A2.2)$$

This cannot always be correct because it amounts to the interchange of an infinite summation and an integration. But certain types of series can be transformed without any error. One of those is described below.

If $F(s)$ is a rational function

$$F(s) = \frac{r_1(s)}{r_2(s)} \qquad (A2.3)$$

in which $r_1(s)$ is of lower degree than the denominator $r_2(s)$, then $F(s)$ can be expanded in partial fractions. If denominator has the simple zeros at $\alpha_1, \alpha_2, \alpha_3, \ldots, \alpha_n, \ldots$

$$r_2(s) = (s-\alpha_1)(s-\alpha_2)(s-\alpha_3)\ldots(s-\alpha_n)\ldots \qquad (A2.4)$$

and

$$F(s) = \sum_{n=1}^{N} \frac{r_1(\alpha_n)}{r_2'(\alpha_n)} \frac{1}{s-\alpha_n} \qquad (A2.5)$$

where $\frac{r_1(\alpha_n)}{r_2'(\alpha_n)}$ are residues at poles α_n. Now, transformation is made term by term and the result is

$$f(t) = \sum_{n=1}^{N} \frac{r_1(\alpha_n)}{r_2'(\alpha_n)} \exp(\alpha_n t) \qquad (A2.6)$$

Laplace inverse transform of function

$$F(s) = \frac{I_0(r\sqrt{s})}{\sqrt{s}\ I_1(\sqrt{s})} \qquad (A2.7)$$

can be obtained using above mentioned series expansion method. The function F(s) of eqn.(2.7) has S explicitly in its denominator, therefore as $s \to \infty$, $F(s) \to 0$. One pole of function F(s) is at zero and other infinite poles are given by

$$I_1(\sqrt{s}) = \frac{1}{i} J_1(i\sqrt{s}) = 0 \qquad (A2.8)$$

or

$$s = -\mu_n^2 \qquad (A2.9)$$

where, μ_n is root of equation

$$J_1(\mu_n) = 0 \qquad (A2.10)$$

Then residues at poles are given as

$$\frac{r_1(\alpha_n)}{r_2'(\alpha_n)} = \frac{I_0(r\sqrt{s})}{\frac{d}{ds}(\sqrt{s}\ I_1(\sqrt{s}))}$$

Taking derivative

$$\frac{r_1(\alpha_n)}{r_2'(\alpha_n)} = \frac{I_0(r\sqrt{s})}{\left\{\frac{1}{2\sqrt{s}} I_1(\sqrt{s}) + \frac{1}{2} I_1'(\sqrt{s})\right\}\Big|_{s=-\mu_n^2}} \qquad (A2.12)$$

Now, since

$$I_o(r\sqrt{s})\Big|_{s\to -\mu_n^2} = I_o(ir\sqrt{s})\Big|_{s\to -\mu_n^2} = J_o(\mu_n r) \qquad (A2.13)$$

$$I_1'(\sqrt{s})\Big|_{s\to -\mu_n^2} = J_1'(i\sqrt{s})\Big|_{s\to -\mu_n^2} = J_1'(\mu_n) \qquad (A2.14)$$

and $$I_1(\sqrt{s})\Big|_{s\to \alpha_n} = 0$$

Above mentioned eqn.(A2.12) for residues reduces to

$$\frac{r_1(\alpha_n)}{r_2'(\alpha_n)} = \frac{2J_o(\mu_n r)}{J_1'(\mu_n)} \qquad (A2.15)$$

Using recurrence relation we obtain

$$J_1'(\mu_n) = J_o(\mu_n) - \frac{J_1(\mu_n)}{\mu_n} \qquad (A2.16)$$

Since, according to eqn.(A2.10), $J_1(\mu_n) = 0$, eqn. (A2.15) reduces to

$$\frac{r_1(\alpha_n)}{r_2'(\alpha_n)} = \frac{2J_o(\mu_n r)}{J_o(\mu_n)} \qquad (A2.17)$$

and

$$\frac{r_1(o)}{r_2'(o)} = \frac{2J_o(ir\sqrt{s})}{J_o(i\sqrt{s})}\Big|_{s=o} = 2 \qquad (A2.18)$$

Hence, Laplace inverse of function F(s), eqn.(A2.7) can be written in the following form with the help of eqns. (A2.6),(A2.17) and (A2.18).

$$f(t) = \frac{r_1(o)}{r_2'(o)} + \sum_{n=1}^{\infty} \frac{r_1(\alpha_n)}{r_2'(\alpha_n)} \exp(\alpha_n t)$$

$$= 2 + \sum_{n=1}^{\infty} 2\frac{J_o(\mu_n r)}{J_o(\mu_n)} \exp(-\mu_n^2 t) \qquad (A2.19)$$

APPENDIX III

The following formula is known as Poisson summation formula Olver (1974), Askay (1975),

$$\sum_{n=0}^{\infty}{}' f(n) = \int_0^{\infty} f(n)dn + 2\sum_{s=1}^{\infty}\int_0^{\infty} f(n)\cos 2\pi s\, n\, d\, n \quad (A3.1)$$

Prime, as a superscript of summation sign, means value of f(n) is half of it, at n = o.

Singular kernel of eqns. (2.20) is given as

$$\sum_{n=1}^{\infty}{}' f(n) = 1+2\sum_{n=1}^{\infty}(-1)^n \cos n\pi x \exp\{-n^2\pi^2(Fo-\tau)\}$$

$$= 2\sum_{n=o}^{\infty}{}'(-1)^n \cos n\pi x \exp\{-n^2\pi^2(Fo-\tau)\} \quad (A3.2)$$

On the application of Poisson summation formula

$$\sum_{n=o}^{\infty}{}' f(n) = 2\left[\int_0^{\infty}(-1)^n \cos n\pi x \exp\{-n^2\pi^2(Fo-\tau)\}dn\right.$$

$$\left. +2\sum_{s=1}^{\infty}\int_0^{\infty}(-1)^n \cos n\pi x \exp\{-n^2\pi^2(Fo-\tau)\}\cos 2\pi sn\, dn\right] \quad (A3.3)$$

On evaluating the integrals

$$\sum_{n=1}^{\infty}{}' f(n) = 2\left[\left\{\frac{1}{4\sqrt{\pi(Fo-\tau)}}\left\{\exp\left\{\frac{(x-1)^2}{4(Fo-\tau)}\right\} + \exp\left\{-\frac{(1-x)^2}{4(Fo-\tau)}\right\}\right\}\right\}\right.$$

$$\left. +2\sum_{s=1}^{\infty}\left\{\frac{1}{4\sqrt{\{\pi(Fo-\tau)\}}}\left\{\exp\left(\frac{(x+2s-1)^2}{4(Fo-\tau)}\right)+\exp\left(\frac{(1+2s-x)^2}{4(Fo-\tau)}\right)\right\}\right\}\right] \quad (A3.4)$$

and then rearranging, we get

$$\sum_{n=1}^{\infty}{}' f(n) = \frac{1}{\sqrt{\{\pi\,(Fo-\tau)\}}}\Big[\exp\{-(x-1)^2/4(Fo-\tau)\} + \sum_{s=1}^{\infty}\exp\{-(x+2s-1)^2/4(Fo-\tau)\} + \exp\{-(1+2s-x)^2/4(Fo-\tau)\}\Big] \tag{A3.5}$$

For the surface, this kernel reduces to

$$\sum_{n=1}^{\infty}{}' f(n) = \Big[1+2\sum_{s=1}^{\infty}\exp\{-s^2/(Fo-\tau)\}\Big]\{\pi(Fo-\tau)\}^{-\frac{1}{2}} \tag{A3.6}$$

Replacing s by n, eqn.(A3.6) can be rewritten as

$$\sum_{n=1}^{\infty}{}' f(n) = \Big[1+2\sum_{n=1}^{\infty}\exp\{-n^2/(Fo-\tau)\}\Big]\{\pi\,(Fo-\tau)\}^{-\frac{1}{2}} \tag{A3.7}$$

APPENDIX IV

Computer programs for successive iteration method and separable kernel method were developed for numerical solution of the nonlinear singular Volterra integral equation. The program is generalised for three simple geometries, i.e. plate, cylinder and sphere distinguished by a variable name IGMTRY.

The computer program is written in Fortran IV. Fortran listing of this program is given in Appendix V.

1. Description of Program:

MAIN program reads various inputs, calls subroutines for surface and centre temperature (step by step) and prints the output data.

The two methods differ in only the way they calculate surface temperature. For separable kernel method subroutine DERIV is called from subroutine SURSKM while, for successive iteration method subroutine GITA is called from subroutine SURSIM.

Subroutine Name	Description
MAIN	It reads all the input, calculates the time step, calls subroutines EPS, SURSKM/SURSIM and CENTRE and prints the output.
SURSKM (used in separable kernel method)	Used for calculating surface temperature. It solves the set of simultaneous differential equations (3.17) by fourth order Runge-Kutta method. It calls subroutine DERIVE.

DERIV	It calculates the derivatives.
SURSIM (used in successive iteration method)	Used for calculating surface temperature by Poission summation formula. It calls subroutine KNOWN and GITA.
GITA	It calculates the last integral in eqn.(3.10) by the Modern Gaussian integration formula.
EPS	It calculates the eigenvalues and other constants.
CENTRE	It calculates the temperature at the centre and for that calls subroutine KNOWN.
BESJ	It calculates the value of Bessel's function of zeroth order.
KNOWN	It evaluates the integral by Simpson's rule.
FLUX	It calculates the outgoing flux corresponding to a nondimensional temperature.

Program Symbol	Definition
ALPHA	Thermal Diffusivity.
BETA	Coefficient of thermal expansion
BETAO	β_o
BETAK	β_k
BMAX	Max.Biot number.
CPF	Thermal capacity of fluid
CPS	Thermal capacity of solid
CPV	Thermal capacity of vapour

CSF	Constant of Nucleate boiling Heat transfer correlation.
D	Thickness of solid
DELT	Small time step
EIGEN	Eigenvalue
EMSVTY	Emissivity of metal
EPSN	ε_M, a constant
FLUX	Outgoing flux
FONO	Fourier number
G	Gravitational constant
GC	Conversion factor
H	Film Heat transfer coefficient
HB	Boiling component in the film boiling
IGMTRY	Geometry of solid
KF	Thermal conductivity of fluid
KS	Thermal conductivity of solid
KV	Thermal conductivity of vapour
L	Height of solid
MUF	Viscosity of fluid
MUV	Viscosity of vapour
N	Number of equations used.
PI	π
PR	Prandtl number
RHOF	Mass density of fluid
RHOS	Mass density of solid

RHOV	Mass density of vapour
SIGMA1	Surface tension
SIGMA2	Steffen Boltzman constant
T	Temperature component
TF	Temperature of fluid
THETA	Nondimensional temperature.
THETAC	Nondimensional temperature at centre
THETAI	Nondimensional temperature corresponding to initial temperature
THETAL	Nondimensional temperature corresponding to Leidenfrost temperature
THETAS	Nondimensional temperature corresponding to saturation temperature
THETAT	Nondimensional temperature corresponding to transition temperature
TINTL	Initial temperature
TLEIDN	Leidenfrost temperature
TSAT	Saturation temperature
TTRANS	Transition temperature
X	Nondimensional value of coordinate
Z	Value of integral.

2. Correlations used in the numerical solution:

a. Film Boiling:

In the film boiling regim heat transfer by radiation dominates over heat transfer by convection.

Boiling heat transfer coefficient h_b is given as

$$h_b = 0.943 \left[\frac{K_v^3 \rho_v (\rho_f - \rho_v) g \lambda'}{L \mu_v (T_s - T_f)} \right]^{\frac{1}{4}} \qquad (A4.1)$$

where $$\lambda' = h_{fg}\left(1 + \frac{0.4 (T_s - T_f) C_{pv}}{h_{fg}}\right) \qquad (A4.2)$$

and total heat transfer coefficient h is given by

$$h = h_b \left(\frac{h_b}{h}\right)^{1/3} + h_r \qquad (A4.3)$$

here h_r is heat transfer coefficient by radiation given as

$$h_r = \sigma \varepsilon \frac{(T_s^4 - T_f^4)}{T_s - T_f}$$

where K_v = Thermal conductivity of vapour

ρ_v = Vapour density

ρ_f = Fluid density

g = Gravitational constant

L = Height of the surface

μ_v = Viscosity of the vapour

C_{pv} = Thermal capacity of vapour

h_{fg} = Latent heat of vapourisation

σ = Steffen Boltzman constant

ε = Emissivity

T_s = Surface temperature

T_f = Fluid temperature.

b. Nucleate Boiling:

Correlation for nucleate boiling heat transfer is

$$\frac{C_{pf}(T_s-T_f)}{h_{fg}\,P_r^{1.7}} = C_{sf}\left[\frac{h(T_s-T_f)}{\mu_f\,h_{fg}}\sqrt{\frac{g_c\,\sigma}{g(\rho_f-\rho_v)}}\right]^{0.33} \qquad (A4.5)$$

where C_{pf} = Thermal capacity of fluid

C_{sf} = A constant

μ_f = Viscosity of fluid

g_c = Conversion factor

σ = Surface tension

c. Free Convection:

The correlation for free convection is

$$Nu = 0.555(GrPr)^{\frac{1}{4}} \qquad (A4.6)$$

where Nu = Nusselt number

Gr = Grashof number

Pr = Prandtl number

3. Input data for numerical solution:

a. Vapour properties (at 100°C):

Density	= 0.598 Kg/m^3
Thermal conductivity	= 0.0249 J/m-°K-sec.
Thermal capacity	= 2.028 KJ/Kg-°K
Viscosity	= 0.0121 mN Sec/m^2
Latent heat of vaporisation	= 2256.94 KJ/Kg

b. Fluid properties (at 100°C):

Density	= 959 Kg/m^3
Thermal conductivity	= 0.669 J/m-°K-Sec
Thermal capacity	= 4.2[illegible] KJ/Kg-°K
Viscosity	= 0.278 mN Sec /m^2
Surface tension	= 58.9 mN/m

c. Fluid properties (at 70°C):
(considered at the mean temperature in free convection regim)

Density	= 990 Kg/m^3
Viscosity	= 0.57 mN Sec/m^2
Coefficient of Thermal expansion	= 0.4×10^{-3} 1/°K
Prandtl number	= 3.6

d. Material properties:

Density	= 7760 Kg/m^3
Thermal conductivity	= 36 J/m-°K-Sec
Thermal Capacity	= 0.486 KJ/Kg-°K
Emissivity	= 0.9

e. Specimen data:

Plate	25 x 25 x 3.7 cms.
Cylinder	20 cms. high, 5.0 cms.diameter
Fluid temperature	= 26°C
Initial temperature for experiments	= 184°C
Initial temperature for the results in Bofor's Handbook	= 900°C.

REFERENCES

1. Askay, R.A. 1975
"Theory and Applications of Special Functions",
Academic Press, New York, p. 148.

2. Burks, A.L., 1966
"Nonsymmetric Heating by Radiation and Convection of an Infinite Plate",
Zh. Prikl, Mekh. Tekh. Fiz., 21, 126-127.

3. Crosbie, A.L. and Banerjee, S.K., 1973,
"Modified Separable Kernel Method for Heat Conduction with a Nonlinear Boundary Condition",
Journal of AIAA, 11, 744-745.

4. Crosbie, A.L. and Banerjee, S.K., 1974.
"Quenching of a Solid Sphere in Oil",
Warme und Stoffubertragung (Therme and Fluid Dynamics),7,113-120.

5. Crosbie, A.L. and Viskanta, R., 1966
"Transient Heating or Cooling of the Dimensional Solids by Thermal Radiation",
Proc. of Third International Heat Transfer Conference,
AICHE, New York, 5, 146-153.

6. Crosbie, A.L. and Viskanta, R., 1968a
"Transient Heating or Cooling of a Plate by Combined Convection and Radiation",
International Journal of Heat and Mass Transfer, 11, 305-317.

7. Crosbie, A.L. and Viskanta, R., 1968b
"A Simplified Method for Solving Transient Heat Conduction Problem with Nonlinear Boundary Conditions",
Journal of Heat Transfer, Vol.C90, 358-359.

8. Devis, P.J. and Polonsky, I., 1965
"Numerical Interpolation, Differentiation and Integration",
Hand-book of Mathematical Functions
Dover Publications, Inc. New York, p. 889.

9. Doetsch, G., 1961
"Table of Laplace Transforms"
Guide to the Applications of Laplace Transforms,
D. Van Nostrand Co.Ltd., London, p. 242.

10. Doetsch, G., 1971
"Series Expansions",
Guide to the Applications of the Laplace and Z-Transforms,
2nd Edition, Van Nostrand Reinhold Co., London, p. 128-137.

11. Fourier, J.B., 1878,
"Theorie Analytique de la Chaleur Oeuvres de Fourier"
Gauthier-Villars, Paris, 1822
English Translation by Freeman, Cambridge, 1878.

12. Gradshteyn, I.S. and Ryzhik, I.W., 1965,
"Theta Function",
Tables of Integrals, Series and Products,
Academic Press, New York, 921-925.

13. Gurney, H.P., and Lurie, J., 1923
"Charts for Estimating Temperature Distributions in Heating or Cooling Solid Shapes",
Ind. Eng. Chem., 15, 1170-1172.

14. Heisler, M.P., 1947
"Temperature Charts for Induction and Constant Temperature Heating",
Trans. ASME, 69, 227-236.

15. Kreith, F., 1965a
"Free Convection",
Principles of Heat Transfer,
2nd Edition, International Text Book Co.Pennsylvania,
p. 356-358.

16. Kreith, F., 1965b
"Heat Transfer with Change in Phase",
Principles of Heat Transfer,
2nd Edition, International Text Book Co., Pennsylvania, p.434-477.

17. Luikov, A.V., 1968
"Boundary Condition of the Second Kind",
Analytical Heat Diffusion Theory,
Academic Press, New York, p. 167-200.

18. Olver, F.W.J., 1974
"Asymptotics and Special Functions",
Academic Press, New York, p. 306.

19. Rajaraman, V., 1974
"Numerical Solution to Differential Equations",
Computer Oriented Numerical Methods
Prentice-Hall International, p. 99.

20. Thelning, K.E., 1975
"Quenching Media",
Steel and its Heat Treatment,
Handbook, Butterworth, London and Boston, p. 219-230.

21. Vidin, Yu.V. and Iganov, V.V., 1965
"Temperature Field in an Infinite Plate Heated Simultaneously by Radiation and Convection",
Izv, Vyssh. Vcheb. Zabed. Avicits. Tekh, 8,4, 3-6.

```
      MAIN PROGRAM

      REAL KV,KF,KS,L,MUV,MUF
      COMMON T(5),FONO(1000),THETA(1000),THETAC,K,DELT
      COMMON EIGEN(50),EPSN,BETAC,BETAK
      COMMON/XW/X(16),W(16)
      COMMON/CONST/C1,C2,C3,C4,C5,C6,C7,B
      COMMON/TEMX/TINTL,TF,THETAL,THETAT,THETAS
C     N FOR NO. OF EQUNS. IN SKM,NO. OF GAUSSIAN ORDER IN SIM
CC    METHOD =1 SUCCESSIVE ITERATION METHOD (SIM)
CC    METHOD =2 SEPARABLE KERNEL METHOD (SKM)
C     READ 100, N,METHOD
CCC   IGMTRY =2 INFINITE CYLINDER
CCCC  IGMTRY =1 INFINITE PLATE

      INPUT  DATA

C
    4 CONTINUE
      PRINT 500
    5 READ 100,IGMTRY
      IF(IGMTRY-1) 70,6,7
    6 PRINT 601
      GO TO 8
    7 PRINT 602
    8 CONTINUE
      READ 400,TINTL,TLEIDN,TTRANS,TSAT,TF
      READ 400, RHOV,KV,MUV,CPV,HFG
      READ 400,RHOF,KF,MUF,CPF,BETA,SIGMA1
      READ 400,RHOS,KS,CPS
      READ 400, G,GC,CSF,SIGMA2,EMSVTY
      READ 400,L,D
C
CCC   EVALUATION OF CONSTANTS
C
      CALL EPS(IGMTRY,N)
      THETAI=(TINTL-TF)/(TINTL-TF)
      THETAL=(TLEIDN-TF)/(TINTL-TF)
      THETAT=(TTRANS-TF)/(TINTL-TF)
      THETAS=(TSAT-TF)/(TINTL-TF)
      ALPHA=KS/(RHOS*CPS)
      PR=CPF*MUF/KF
      C1=HFG
      C2=0.4*CPV*(TINTL-TF)
      C3=0.943*(KV**3*RHOV*(RHOF-RHOV)*G/(L*MUV*(TINTL-TF)))**.25
      C4=SIGMA2*EMSVTY
      C5=((CPF/(CSF*HFG*PR**1.7))**3)*(TINTL-TF)**2*MUF*HFG*SQRT(G*(RHOF
     1 -RHOV)/(GC*SIGMA1))
      READ 400, PR,RHOF,BETA,MUF
      C6=.021*(PR*RHOF**2*BETA*G*(TINTL-TF)/MUF**2)**0.4*L**0.2
      C7=(D/2.)/KS
      PRINT 700
C
CCC   INITIATING THE  CALCULATION
C
      TT=1.
      J=2
      GTT=FLUX(J,TT)
      BMAX=B
      DELTIN=.001/BMAX
      DELT=DELTIN
```

```
      FONC(1)=DELT
      THETA(1)=1.
      THETAC=1.
      T(1)=1.
      DO 10 I=2,N
   10 T(I)=0.
      K=0
   20 CONTINUE
      K=K+1
      IF(METHOD.EQ.2) GO TO 21
      CALL SIRSIM(N)
      TEMP=THETA(K)
      GO TO 31
   21 CALL SURSKM(N)
      TEMP=0.
      DO 30 I=1,N
   30 TEMP=TEMP+T(I)
      THETA(K)=TEMP
   31 CONTINUE
      CALL CENTRE
   40 CONTINUE
      PRINT 200, FONC(K),THETA(K),THETAC
   50 CONTINUE
      IF(FONO(K).GE.5..OR.TEMP.LE..1) GO TO 60
      GTT=FLUX(TEMP)
      DELT=DELTIN*(BMAX/B)**2
      FONO(K)=FONO(K-1)+DELT
      GO TO 20
   60 CONTINUE
      GO TO 5
   70 CONTINUE
      STOP
  100 FORMAT( 20I4)
  200 FORMAT(10X,E12.5,5X,F8.5,5X,F8.5)
  300 FORMAT(//F12.7,I4//)
  400 FORMAT(6E12.5)
  500 FORMAT(1H1,*   GENERAL PROGRAMME FOR SURFACE TEMP. FOR ANY GEOMETRY
     1Y BY SEPARABLE KERNEL METHOD*)
  601 FORMAT(//10X,*GEOMETRY -- INFINITE PLATE*/)
  602 FORMAT(//10X,*GEOMETRY -- INFINITE CYLINDER*/)
  700 FORMAT(16X,*FONO*,7X,*TEMPS*,5X,*TEMPC*//)
      END



      SURSKM(N)
      COMMON T(5),FONO(1000),THETA(1000),THETAC,K,DELT
      COMMON EIGEN(50),EPSN,BETAC,BETAK
      DIMENSION S(5),S1(5),S2(5),S3(5),S4(5)
      DO 10 I=1,N
   10 S(I)=0.
      CALL DERIV(N,0.,S,S1)
      CALL DERIV(N,.5,S1,S2)
      CALL DERIV(N,.5,S2,S3)
      CALL DERIV(N,1.,S3,S4)
      DO 20 I=1,N
   20 T(I)=T(I)+DELT*(S1(I)+2.*S2(I)+2.*S3(I)+S4(I))/6.
      RETURN
      END
```

```
      SUBROUTINE DERIV(N,C,S,SS)
      COMMON T(5),FONO(1000),THETA(1000),THETAC,K,DELT
      COMMON EIGEN(50),EPSN,BETAO,BETAK
      DIMENSION S(5),SS(5)
      TT=0.
      DO 10 I=1,N
   10 TT=TT+T(I)+S(I)*DELT*C
      GTT=FLUX(TT)
      X=FONO(K)+DELT*C
      Y=T(I)+S(I)*DELT*C
      DO 60 I=1,N
      IF(I-1) 60,30,20
   20 IF(I-N) 40,50,60
   30 SS(I)=-BETAO*GTT
      GO TO 60
   40 SS(I)=-BETAK*GTT-EIGEN(I-1)**2*Y
      GO TO 60
   50 SS(I)=-EPSN*BETAK*GTT-EIGEN(I-1)**2*Y
   60 CONTINUE
      RETURN
      END
```

```
      SUBROUTINE EPS(IGMTRY,N)
      COMMON T(5),FONO(1000),THETA(1000),THETAC,K,DELT
      COMMON EIGEN(50),EPSN,BETAO,BETAK
      N1=N-1
      N2=N-2
      GO TO (100,200,300),IGMTRY
  100 BETAO=1.
      BETAK=2.
      PI=3.1415927
      DO 110 I=1,N1
  110 EIGEN(I)=PI*FLOAT(I)
      EPSN=1./3.
      GO TO 400
  200 BETAO=2.
      BETAK=2.
      EIGEN(1)=3.8317
      EIGEN(2)=7.0156
      EIGEN(3)=10.1735
      EIGEN(4)=13.3237
      DO 210 I=5,N1
  210 EIGEN(I)=FLOAT(I)*PI+PI/4.
      EPSN=.25
      GO TO 400
  300 CONTINUE
  400 CONTINUE
      DO 420 I=1,N2
  420 EPSN=EPSN-BETAK/EIGEN(I)**2
      EPSN=EPSN*EIGEN(N1)**2/BETAK
      RETURN
      END
```

```
      SUBROUTINE SUBSIN(N)
      COMMON T(5),FONO(1000),THETA(1000),THETAC,K,DELT
      COMMON EIGEN(50),EPSN,BETA0,BETAK
      COMMON/XW/X(16),W(16)
      DIMENSION POISUM(16)
      REAL INTFUN
      THETAN=1.
      IF(K.NE.1) THETAN=THETA(K-1)
      DO 120 I=1,N
      S=0.
      M=1
  110 CONTINUE
      POISUM(I)=S+EXP(-FLOAT(M)**2/(DELT*X(I)**2))
      IF(ABS(POISUM(I)-S).LT..001) GO TO 115
      S=POISUM(I)
      M=M+1
      GO TO 110
  115 CONTINUE
  120 CONTINUE
C     TAKING FIRST APPROXIMATION OF THETA(K)=THETAN
      THETA(K)=THETAN
      CALL KNOWN(Z)
      M=1
  300 CONTINUE
      CALL GITA(N,INTFUN,POISUM)
      S=Z-INTFUN
      IF(ABS(THETA(K)-S).LT.(.00001*THETA(K)) GO TO 400
      THETA(K)=S
      M=M+1
      GO TO 300
  400 COUNTINUE
      RETURN
      END


      SUBROUTINE GITA(N,INTFUN,POISUM)
      COMMON T(5),FONO(1000),THETA(1000),THETAC,K,DELT
      COMMON EIGEN(50),EPSN,BETA0,BETAK
      COMMON/XW/X(16),W(16)
      REAL INTFUN
      J=1
      PI=2.*ARSIN(1.)
      H=0.
      DO 10 I=1,N
      Q=FLUX(J,TEMP)
      H=H+W(I)*(1.+2.*POISUM(I))*Q
   10 CONTINUE
      INTFUN=2.*SQRT(DELT/PI)*H
      RETURN
      END


      SUBROUTINE CENTRE
      COMMON T(5),FONO(1000),THETA(1000),THETAC,K,DELT
      COMMON EIGEN(50),EPSN,BETAC,BETAK
      CALL KNOWN(Z)
      RETURN
      END
```

```
      SUBROUTINE KNOWN (Z)
      COMMON T(5),FONO(1000),THETA(1000),THETAC,K,DELT
      COMMON EIGEN(50),EPSN,BETAC,BETAK
      M=K
      X=0.
      J=2
      PI=2.0*ARSIN(1.0)
      Z=0.
      IF(M.LE.1) GO TO 60
      M1=M-1
      DO 50 I=1,M1
      Z1=1.
      IF(I-1) 60,10,20
10    TAU=0.5*FONO(1)
      GO TO 21
20    TAU=FONO(I)-0.5*(FONO(I)-FONO(I-1))
21    CONTINUE
      K=1
      ZZ=-1.
29    CONTINUE
      EI=EIGEN(K)
      IF(IGMTRY-2) 30,31,32
30    CONTINUE
      Z2=Z1+2.*ZZ*EXP(-EI**2*(FONO(M)-TAU))
      GO TO 32
31    CALL BESJ(EI,0,BJ,.001,IER)
      Z2=Z1+2.*(1./BJ)*EXP(-EI**2*(FONO(M)-TAU))
32    CONTINUE
      IF(ABS(Z2-Z1).LT.(.01*Z2)) GO TO 40
      Z1=Z2
      K=K+1
      ZZ=-ZZ
      GO TO 29
40    CONTINUE
      IF(I-1) 60,41,42
41    TEMP=(1.+THETA(1))/2.
      GO TO 43
42    TEMP=(THETA(I-1)+THETA(I))/2.
43    CONTINUE
      Q=FLUX(J,TEMP)
      Z=Z+Z2*Q*DELT
50    CONTINUE
60    CONTINUE
      Z=1.0-Z
      RETURN
      END
```

```
      SUBROUTINE BFSJ(X,N,BJ,D,IER)
C     SUBROUTINE FOR ZEROTH ORDER ONLY
      IF(N.NE.0) GO TO 20
      X2=(X/2.)**2
      BJ=1.
      X3=1.
      K=1
    1 X3=-X3*X2/FLOAT(K)**2
      X4=X3
      K=K+1
      X3=-X3*X2/FLOAT(K)**2
      X4=X4+X3
      BJ=BJ+X4
      IF(ABS(X4).LE.ABS(D*BJ)) GO TO 20
      K=K+1
      GO TO 1
    2 CONTINUE
      RETURN
      END



      FUNCTION FLUX(J,TT)
      COMMON/CONST/C1,C2,C3,C4,C5,C6,C7,B
      COMMON/TEMX/TINTL,TF,THETAL,THETAT,THETAS
      REAL LEMDA
      GO TO (1,2),J
    1 TT=1.+(THETA(K)-1.)*(1.-X(I)**2)
      IF(K.NE.1) TT=THETA(K-1)+THETA(K)-THETA(K-1))*(1.-X(I)**2)
    2 CONTINUE
      IF(TT.LE.THETAL) GO TO 10
      LEMDA=C1+C2*TT
      HB=C3*(LEMDA/TT)**0.25
      HR=C4*((TT*(TINTL-TF)+TF+273.)**4-(TF+273.)**4)
      H=HB+HR
      H=HB*(HB/H)**(1./3.)+HR
      B=C7*H
      FLUX=B*TT
      RETURN
   10 IF(TT.LE.THETAT) GO TO 20
      GO TO 20
   15 CONTINUE
      RETURN
   20 IF(TT.LE.THETAS) GO TO 30
      H=C5*TT**2
      B=C7*H
      FLUX=B*TT
      RETURN
   30 CONTINUE
      H=C6*TT**0.4
      B=C7*H
      FLUX=B*TT
      RETURN
      END
```